

# Reduced cell death, invasive and angiogenic features conferred by BRCA1-deficiency in mammary epithelial cells transformed with H-Ras

Arunasalam Navaraj,<sup>1</sup> Niklas Finnberg,<sup>1</sup> David T. Dicker,<sup>1</sup> Wensheng Yang,<sup>1</sup> Elizabeth M. Matthew<sup>1</sup> and Wafik S. El-Deiry\*

<sup>1</sup> Laboratory of Molecular Oncology and Cell Cycle Regulation, Departments of Medicine (Hematology/Oncology), Genetics and Pharmacology, the Institute for Translational Medicine and Therapeutics, and The Abramson Comprehensive Cancer Center, University of Pennsylvania School of Medicine, Philadelphia, PA

**Key words:** breast cancer, BRCA1, p53, H-Ras, apoptosis, angiogenesis, EMT, imaging, invasion

**Abbreviations:** HMEC, human mammary epithelial cell; BRCA1, breast cancer gene 1; shRNA, short hairpin RNA; MAPK, mitogen activated protein kinase; MMP, matrix metallo proteases; EMT, epithelial to mesenchymal transition

To investigate the role of tumor suppressors BRCA1 and p53 proteins in human breast tumorigenesis, we transformed immortalized human mammary epithelial cells, MCF10A, with or without BRCA1/p53 gene-specific knockdowns. Stable knockdown of BRCA1 alone in MCF10A cells led to centrosome amplification, impaired p53 protein stability, increased sensitivity towards DNA-damaging agents, defective chromosomal condensation at mitosis and elevated protein levels of cyclin D1 and c-myc. While over-expression of mutant H-Ras transformed MCF10A cells, depletion of BRCA1 dramatically enhanced the *in vivo* tumorigenesis that was associated with higher levels of VEGF, enhanced vascularization and less apoptosis in the BRCA1-deficient Ras-transformed tumors. The Ras-transformed BRCA1-deficient tumors exhibited features of the epithelial-to-mesenchymal transition, appeared to secrete matrix metalloproteases as visualized by *in vivo* bio-imaging of tumors using fluorescent probe MMP680, and were locally metastatic to lymph nodes. Our results suggest that loss of BRCA1 function may contribute to the aggressiveness of Ras-MAPK driven human breast cancer with associated increase in levels of cyclin D1 and c-myc, enhanced MAPK activity, angiogenic potential & invasiveness. This mammary xenograft tumor model may be useful as a tool to understand human breast tumor angiogenesis and metastasis, as well as to test candidate therapeutics.

## Introduction

Human mammary epithelial cells (HMECs) such as luminal, myoepithelial and basal have a finite lifespan and undergo senescence in culture.<sup>1,2</sup> The initial steps in tumorigenesis involve the loss of senescence control and immortalization. Cell culture models have helped in identifying many gene alterations leading to HMEC immortalization and in understanding the biology of early breast cancer.<sup>1,3</sup> Malignant cellular transformation is a complex multistep process that is associated with inactivation of tumor suppressors and activation of different oncogenes depending on cell type.<sup>4-6</sup> Use of different combinations of oncogenic expressions has resulted in efficient transformation of normally senescing HMEC's into aggressive breast cancer cells *in vivo*.<sup>7</sup> Deletion of tumor suppressor genes in transgenic mouse models has also contributed to the understanding of breast cancer progression.

Over a decade ago, genetic linkage analysis and positional cloning identified the BRCA1 gene on human chromosome 17q21<sup>8,9</sup> and mutations have been found to account for nearly 50% of hereditary breast cancer cases and almost all

hereditary ovarian cancer cases.<sup>9,10</sup> Despite its tissue specificity, this 1,863-amino-acid protein has universal roles in DNA repair, cell cycle control, chromatin remodeling, transcriptional regulation, centrosome amplification, genome/protein stability, and X-chromosome inactivation.<sup>11-15</sup> Interestingly, breast tumors from BRCA1 germ-line mutation carriers frequently display allelic losses at other major tumor suppressor loci such as p53 and PTEN and increased expression of c-myc and ErbB2.<sup>16,17</sup> These findings indicate a genetic and biochemical co-operativity between BRCA1 and other tumor suppressors and oncogenes.

To understand the role of BRCA1 and p53 in human mammary epithelial cell transformation and breast tumorigenesis, we transformed human mammary epithelial MCF10A cells using mutant H-Ras and also introduced stable RNA interference (RNAi) targeting the tumor suppressors through retroviral mediated gene specific-shRNA expression. Depletion of BRCA1 in H-Ras transformed MCF10A xenograft tumors resulted in larger soft agar colonies, aggressive tumor formation *in vivo*, larger size tumors with lesser apoptosis, increased levels of VEGF and blood vessel formation. In contrast, depletion of p53 in H-Ras transformed MCF10A xenograft tumors did not

\*Correspondence to: Wafik S. El-Deiry; Email:

Submitted: 12/3/09; Revised: 12/13/09; Accepted: 12/14/09

Previously published online: [www.landesbioscience.com/journals/cbt/article/10850](http://www.landesbioscience.com/journals/cbt/article/10850)

show much enhancement in tumor growth *in vivo*. Interestingly, blocking the two major tumor suppressors, BRCA1 and p53 either alone or in combination was not sufficient to transform a normal mammary epithelial cell into a cancer cell. These findings suggest that apart from blocking BRCA1/p53 functions, the mammary epithelial cells also need further hits such as oncogenic activation which may be provided by the loss of genomic stability, to transform a normal cell into a breast cancer cell.

## Materials and Methods

**Generation of stable knock-down cell lines.** Non-transformed human breast epithelial MCF10A cells were grown as described before.<sup>18</sup> For BRCA1 shRNA, a 64-mer oligonucleotide with the target sequence of 5'-GGCTACAGAAACCGTGCCAAA-3'<sup>19</sup> was synthesized with BamHI and EcoRI overhang and cloned into BamHI and EcoRI sites of pSiren Retro Q (Clontech) having marker ZS-Green. pBABE-puro-Ras-V12 was a kind gift of Dr. Robert Weinberg (Whitehead Institute for Biomedical Research, Cambridge, MA). Construction of pKS-neo-Luc was described previously.<sup>20</sup> Amphotrophic retroviruses were made by transfecting Phoenix-Ampho cells with the Lipofectamine2000 reagent (Invitrogen) by following the manufacturer's instructions. After 2 days of transfection, the filtered viral supernatant was used to infect target MCF10A cells using spin centrifugation.<sup>21,22</sup> Retroviruses were infected serially and cells over expressing Luciferase or H-Ras V12 were selected either with 200 µg/mL neomycin or 1 µg/mL puromycin respectively or FACS sorted for zs-green or RFP positive samples, over expressing shRNAs specific for BRCA1 and p53, respectively.

**In vivo bioluminescence imaging of tumors, internal organs and isolation of tumor cells.** Immunodeficient BALB/c nude mice were injected subcutaneously either in flanks or in mammary fat pads with cell suspension prepared in 50% Matrigel. For each cell line, a total of ten mice were injected with 10 million cells/injection. *In vivo* tumor growth was monitored by imaging mice at regular time intervals using the Xenogen *In Vivo* Imaging System (Xenogen, Alameda, CA). Mice were imaged 5–10 min after intraperitoneal injection of D-luciferin (5 mg/mouse) combined with ketamine/xylazine as the anesthetic drug combination. For imaging the internal organs, tumor-bearing mice were sacrificed after 10 min of ketamine/xylazine injection, and different organs were harvested quickly and imaged for either luciferase or zs-green expression using appropriate filters.

For MMP680 imaging, 2 nmol probe was injected retro-orbitally into tumor-bearing mice. Animals were imaged at different time intervals using the CRi Maestro *in vivo* imaging system and spectral unmixing was performed to subtract the background autofluorescence. The same approach was used to detect zs-green expression in different internal organs using appropriate filters after sacrificing the animals and harvesting the organs.

For isolating cells, tumor tissues were washed in PBS and digested with 1 mg/ml collagenase A for 2 hr at 37°C. The tissue mixture was dispersed using an 18-gauge needle and plated in DMEM:F12 growth medium containing the essential supplements.

**Immunoblotting, immunofluorescence and histology.** Protein lysates were separated using either 15% SDS-Polyacrylamide gels for lower molecular weight proteins or using 8% gels for higher molecular weight proteins. After separation, proteins were transferred from the gels onto a PVDF membrane, blocked with 5% milk proteins for 1 hr at room temperature and probed with different primary antibodies overnight at cold room. Primary antibodies included p53 (sc-126 HRP), phospho (serine-15) p53 (Cell Signaling, 9286), BRCA1 (Santa Cruz, sc-642), p21 (Calbiochem, OP64), EGFR (Cell Signaling, 2646), HER-2 (Santa Cruz, sc-284), c-myc (sc-764), cyclin D1 (Calbiochem CC11), Ras (sc-35), VEGF (sc-152), p44MAPK (Cell Signaling, 9102), phospho MAPK (Cell Signaling, 9101), Ran (BD Transduction Laboratories, 610341), DR5 (Cell Signaling, 3696), BAX (Cell Signaling, 2774), PUMA (Calbiochem, PC-686), β-Tubulin (SC-5274), E-Cadherin (BD Biosciences, 610181), β-Catenin (BD Biosciences, 610153), Vimentin (Novus Biologicals, NB200-621) and α-Smooth Muscle Actin (Sigma, A2547). After primary antibody incubation, blots were washed thrice in TBS-T, incubated with proper secondary antibodies for 2 hours at room temperature, washed again in TBS-T three times and developed with ECL reagent.

Cells were grown in chamber slides overnight to confluency, fixed with acetone:methanol (1:1 ratio) for 20 min on ice, treated with 0.5% Triton X-100 and blocked with 4% goat serum. Cells were incubated with primary antibodies at appropriate dilutions in PBS containing 0.1% Triton X-100 overnight, washed with PBS containing 0.1% Triton X-100 three times, incubated with corresponding cy-3 conjugated secondary antibodies in PBS containing 0.1% Triton X-100 for 2 hr at room temperature and again washed three times as mentioned above. Cells were treated with diluted DAPI before mounting the slides with cover slips for viewing under microscope. Primary antibodies included γ-Tubulin (Sigma, T3559), E-Cadherin (BD Biosciences, 610181), β-Catenin (BD Biosciences, 610153), Vimentin (Novus Biologicals, NB200-621), α-Smooth Muscle Actin (Sigma, A2547), γH2AX (Upstate, 07-164) and Phospho-ATM (Rockland, 200-301-500).

Tumor tissues were harvested after sacrificing mice and immediately fixed in 4% paraformaldehyde overnight at 4°C and paraffin sections were made. Immunohistochemistry was performed by dewaxing and rehydrating slides and subjecting them to antigen retrieval through boiling in 1mM citric acid buffer (pH 6.0) for 15 min. To quench endogenous peroxidases, 2% hydrogen peroxide was used and an avidin/biotin blocking kit (Vector Laboratories, Burlingame, CA) was used to inhibit endogenous biotin, followed by protein blocking (Coulter Immunotech, Marseille, France). Sections were incubated with different primary antibodies overnight, followed by PBS washes, incubation with biotinylated secondary antibodies (Vector Laboratories), developed with 3,3'-diaminobenzidine kit (Vector Laboratories) and counter stained with hematoxylin. Representative depiction of histology and immunohistochemistry was made using the IP Lab software. Primary antibodies included Ki-67 (Oncogene Research Products, NA59), VEGF (Santa Cruz, sc-152), CD34 (Abcam, ab8158), E-Cadherin

(BD Biosciences, 610181),  $\beta$ -Catenin (BD Biosciences, 610153), Vimentin (Novus Biologicals, NB200-621),  $\alpha$ -Smooth Muscle Actin (Sigma, A2547)

**Anchorage-independent and trans well migration assay.** Anchorage independent soft agar assays, a bottom layer of 0.5% noble agar in DMEM:F12 (1:1 ratio) without serum was first placed in 6 cm dishes. Different MCF10A cells were seeded in 0.3% top agar having serum and other growth supplements. Fresh top agar was added every 4th day and colonies were monitored up to 30 days after seeding.<sup>7</sup> Trans well migration assay was performed as described.<sup>23</sup>

**Metaphase spreads.** Exponentially growing cells were arrested with colcemid (0.02  $\mu$ g/mL; Sigma) and processed further before dropping onto ice-cold glass slides and air dried as described before.<sup>20</sup>

**TUNEL staining for apoptosis in tumors.** TUNEL staining was done as mentioned in manufacturer's protocols (Chemicon, cat # S7165).

## Results

**Construction and characterization of stable BRCA1 and p53 shRNA knockdown in MCF10A cells with mutant H-Ras over-expression.** We stably over-expressed firefly luciferase through retroviral-mediated transduction of MCF10A cells for imaging purposes, selected for neomycin resistance and referred to the cells hereafter as ML (MCF10A-Luc) cells. To investigate the role of BRCA1 and p53 in human mammary epithelial cell transformation, we generated different retroviral vectors that expressed gene-specific shRNA to stably knockdown the expression of both BRCA1 and p53 in ML cells, either separately or together. These cells were selected for *zs-green* expression for BRCA1 knockdown or for RFP expression for p53 knock down by FACS, and referred as MLB (MCF10A-Luc-BRCA1 knockdown) and MLP (MCF10A-Luc-p53 knockdown, **Fig 1a and 1b**). Western blot analysis confirmed the effective and stable knockdown of BRCA1 and p53 in MLB and MLP cells (**Fig 1aii and Fig 1bii**). As a way of characterizing these cells for different biological defects with stable BRCA1 knockdown, centrosomal staining using  $\gamma$ -tubulin antibody and giemsa staining after colchicine-induced mitotic arrest were carried out.<sup>14,24</sup> The presence of highly decondensed mitotic chromosomes and multiple centrosomes confirmed the BRCA1 deficiency leading to altered cellular functions in these MLB cells (**Fig 1aiii and 1aiv**). Earlier work from our laboratory had shown the importance of BRCA1 in mediating p53 stability.<sup>15</sup> As expected, in BRCA1 deficient MLB cells, p53 stability was drastically impaired when cells were treated with DNA-damaging agents (**Fig 1biii**).

Ever since the first demonstration of successful human cellular transformation using an oncogenic, mutant Ras (H-RasV12) in combination with other oncogenes like SV40 T-Ag and h-TERT to convert a normally senescing fibroblast into a highly malignant cancer cell,<sup>25</sup> the H-RasV12 has been used in many studies to effectively transform different cell lines including human mammary epithelial cells.<sup>7</sup> After constructing the stable knockdown cell line for both BRCA1 and p53, those MLB and MLP cells

were subsequently transduced with mutant H-RasV12 retroviral vectors, selected for puromycin and called MLR (MCF10A-Luc-Ras), MLBR (MCF10A-Luc-BRCA1knockdown-Ras), MLPR (MCF10A-Luc-p53knockdown-Ras) and MLBPR (MCF10A-Luc-BRCA1/p53knockdown-Ras) (**Fig 1c**). Interestingly as shown before for efficient mammary epithelial cell transformation,<sup>7</sup> using the hygromycin marker for selecting Ras expressing ML cells (Hygro-Ras) resulted in lesser Ras protein levels and weaker downstream MAPK signaling compared to higher Ras levels and stronger MAPK signaling in cells selected for puromycin marker (Puro-Ras) (**Fig 1cii**). So, we chose to use puro-Ras cells for all our further studies. Western analysis of different protein levels in those mutant Ras over-expressing MLBR, MLPR and MLBPR cells showed higher levels of c-myc, cyclin D1, EGFR and Her-2. Surprisingly, elevated levels of those proteins were observed in BRCA1-knockdown (MLB) cells also without any mutant Ras expression. But, in cells with p53 knockdown alone (MLP) the levels of those oncogenic proteins remained the same as in control ML cells (**Fig 1ciiii**). Growth measurement of these cells in vitro showed an increase in growth rate when cells lacked BRCA1 (**Fig 1d**). This enhanced growth rate of BRCA1 deficient cells in vitro may be due to impaired differentiation process and enhanced proliferation.<sup>19</sup>

**Enhanced Ras-mediated transformation with BRCA1 depletion.** One of the hallmarks of transformed cells is the ability to grow in an anchorage-independent manner in soft agar. When different ML cells were plated in soft agar, only mutant Ras-expressing cells were able to grow and form colonies whereas cells lacking mutant Ras did not form any colony (**Figure 2ai** and complete data not shown). Interestingly, this Ras-mediated transformed phenotype was much enhanced with higher colony number in soft agar assays when BRCA1 was also depleted (**Fig 2aii**). Visible colonies were observed as early as ten days after seeding the cells in soft agar with BRCA1 knockdown whereas knocking down p53 did not enhance colony formation in soft agar assays.

Mammary epithelial cells grown in three-dimensional (3D) matrigel culture can resemble breast epithelium in vivo including formation of spherical acini with apicobasal polarization of cells surrounding a hollow lumen.<sup>26,27</sup> The mechanism and signaling pathways dictating individual cells to arrange into a polarized glandular architecture are still unclear. Thus, the three-dimensional culture of mammary epithelial cells provides a model to investigate the biological activities of genes associated with breast cancer. To study the changes in BRCA1-depleted and/or Ras over-expressing ML cells, they were grown in matrigel matrix as described<sup>26</sup> and monitored at different time intervals as shown in **Fig 2aiii**. Control ML cells formed organized acini with a single layer of luminal cells surrounding a hollow lumen. By contrast, Ras over-expressing MCF10A-Luc (MLR) cells formed large irregular-shaped multilobular structures with a filled lumen. In BRCA1-depleted, Ras over-expressing (MLBR) cells, these unusual structures were observed as early as the second day after seeding the cells on matrigel (**Figure 2aiii**).

To test the tumorigenic potential of these cell lines in vivo, each cell line was injected into immunodeficient nude mice

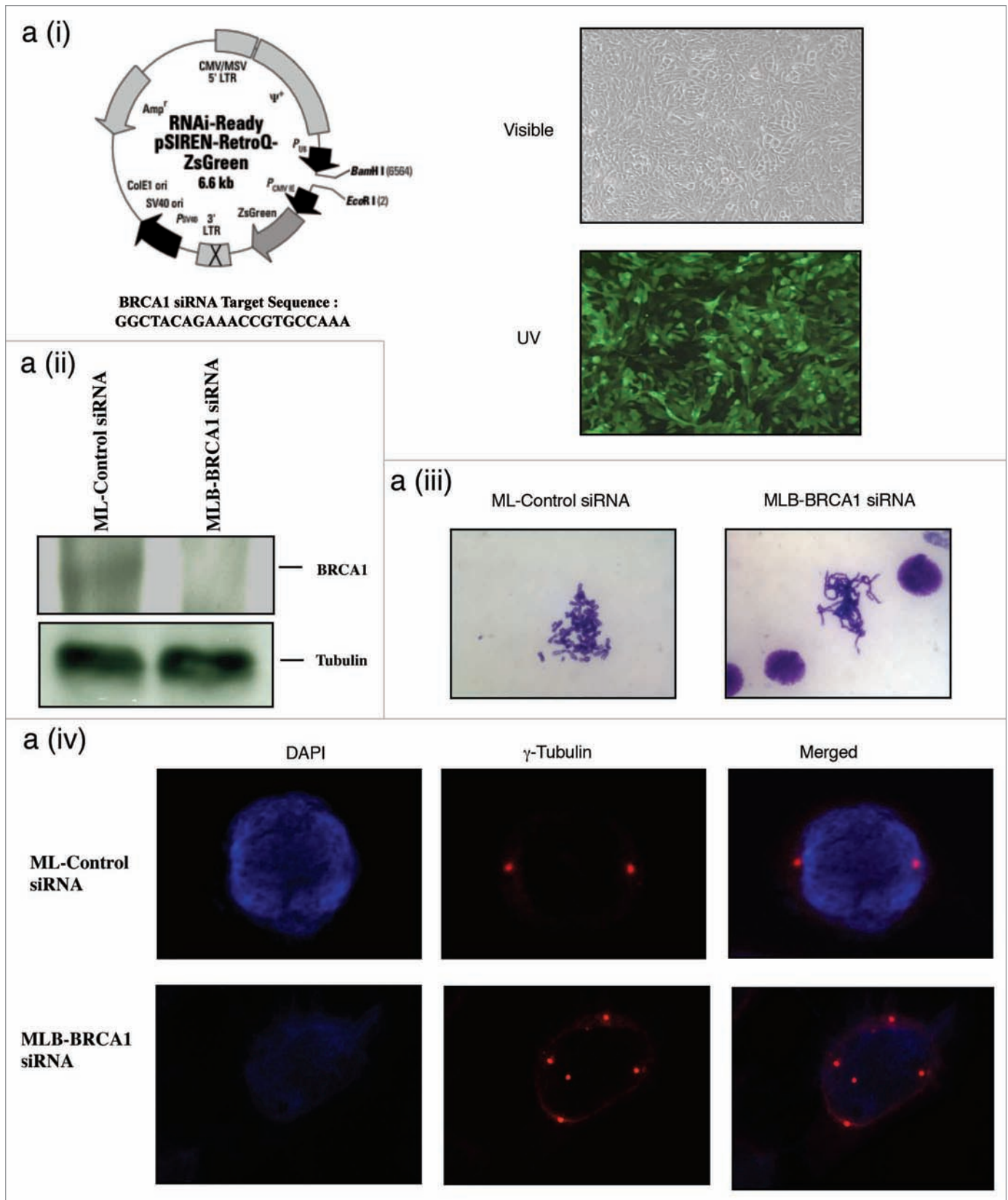


**Figure 1a.** For figure legend, see page 116.

**Figure 1a.** Generation of MCF10A cells with knockdown of BRCA1, p53 and transformation by mutant H-Ras. 1a. Construction and characterization of BRCA1 stable siRNA knockdown in MCF10A-Luc cells. The retro viral vector map used to clone the annealed double stranded siRNA oligo into BamH I and EcoR I sites. Retro viruses were prepared, the target MCF10A-Luc cells were infected as mentioned in materials and methods and sorted for BRCA1 knock down with zs-green selection marker by FACS (**Fig 1ai**). Western blot analysis of BRCA1 knockdown (**Fig 1aii**), metaphase chromosome spread (**Fig 1aiii**) and centrosomal staining using  $\gamma$ -Tubulin antibody (**Fig 1aiv**) were done to confirm the biological defects of BRCA1 deficiency.

**Table 1.** Summary of tumor formation using different MCF10A-Luc-Ras transformed cells injected into nude mice. The tumor # incidence represents the single tumor observed at each injection site for which there was only one injection of cells/site

	Tumor #/# of injections (Flank Region)	Tumor #/# of injections (Mammary Fat Pad)
MCF10A-Luc (ML)	0/10	n.d.
MCF10A-Luc-BRCA1 KD (MLB)	0/10	n.d.
MCF10A-Luc-p53 KD (MLP)	0/10	n.d.
MCF10A-Luc-BRCA1-p53 KD (MLBP)	0/10	n.d.
MCF10A-Luc-Ras (MLR)	6/10	0/30
MCF10A-Luc-BRCA1 KD-Ras (MLBR)	6/10	15/30
MCF10A-Luc-p53 KD-Ras (MLPR)	5/10	n.d.
MCF10A-Luc-BRCA1-p53 KD-Ras (MLBPR)	5/10	n.d.

n.d.=not determined

subcutaneously in the flank region. In order to detect the growth of tumor tissue in nude mice and to quantify the bioluminescence signal as a measure of tumor growth *in vivo*, the firefly luciferase gene was used as a marker. By measuring the bioluminescence signal, we could detect the tumor cell growth kinetics even before formation of a visible tumor as the injected and viable cells were the only source of luciferase activity in the mice. In each individual animal, two injections were made. On the left side of the animal we injected cells having normal levels of BRCA1 as a control and on the right side of the animal we injected cells having depleted levels of BRCA1 (eg. injection of MLR and MLBR on left and right sides of the same individual animal, or MLPR and MLBPR on left and right sides of an animal, respectively). We detected a strong luciferase signal after three days of injecting different cell lines. Though bioluminescence signal from tumors having normal levels of BRCA1 showed a slight decrease for the initial few weeks, later on it showed an increase. By contrast, the xenografted tumors with deficient levels of BRCA1 (both MLBR and MLBPR) showed much enhanced growth. The most aggressively growing tumor resulted with injection of MLBR cells. Small tumor nodules were identified at 25 days post injection and 6 tumors with much higher luciferase signal ( $>1 \times 10^9$  photons/second) were formed by 40 days from 10 different injections (Table 1). Surprisingly, depletion of p53 did not appear to enhance the xenograft tumor growth *in vivo* whereas BRCA1 knockdown drastically enhanced the Ras-transformed tumor growth in mice (Fig 2bi and Fig 2bii). MCF10A cell lines having depleted levels of BRCA1 and/or p53 proteins failed to form any tumor in the absence of H-RasV12 expression (data not shown). The xenografted tumors with deficient levels of BRCA1 were much bigger in size than tumors with wild type levels of BRCA1 (Fig 2biii and Fig 2biv). Western blot analysis of these xenografted tumor tissues confirmed the depleted levels of tumor suppressors, BRCA1 and p53 with respective shRNA expression and higher levels of Ras oncoprotein with enhanced

MAPK activation (Fig 2ci and 2cii). Unexpectedly, the Ras oncoprotein showed a slight mobility shift only in tumor tissues (lanes 6 and 7 in Fig 2ci). Interestingly, p53 protein levels were reduced even in xenografted tumors having no p53-specific shRNA expression (lanes 2-3 and lanes 6-7 in Fig 2ci). In many of the BRCA1-associated familial breast cancer, the p53 gene is also mutated at unique spots not found in other types of cancer.<sup>28</sup> So, we were interested in testing the levels of p53 protein in Ras-transformed cells (MLR and MLBR), in the corresponding tumor xenografts and in the cell lines re-established from those tumor xenografts. Surprisingly, p53 expression was greatly reduced only in tumor xenografts that formed *in vivo* whereas the corresponding transformed cells retained p53 expression though BRCA1 depletion led to reduced p53 stability. When levels of a few of the pro-apoptotic downstream targets of p53 were analyzed, we found only in tumor tissues a complete loss of DR5 expression and reduction in BAX level but the levels of PUMA remained unchanged in tumor tissues (Fig 2d).

**Histological analysis of BRCA1 depleted Ras-transformed mammary tumor xenografts.** As BRCA1 deficiency led to aggressive growth of xenografted tumors *in vivo* with increased size and mass (Fig 2bi-Fig 2biv), we were interested in analyzing the proliferation and apoptosis occurring in the tumors. We speculated that reduction of both p53 and its downstream pro-apoptotic targets like DR5 and BAX in tumor xenografts may result in reduced apoptosis. As a marker of proliferation, the tumor xenograft sections were stained for Ki-67 and TUNEL staining was performed to detect apoptosis. Ki-67 staining of both tumor tissues having either normal levels or depleted levels of BRCA1 showed little difference in proliferation of cells in those growing tumors *in vivo* (Fig 3ai and 3aii). Surprisingly, TUNEL staining showed more than a two-fold decrease in apoptosis in tumor tissues with depleted levels of BRCA1 (Fig 3bi and 3bii). These results suggested that in the absence of functional BRCA1 protein, the tumor tissues lacked the ability to undergo

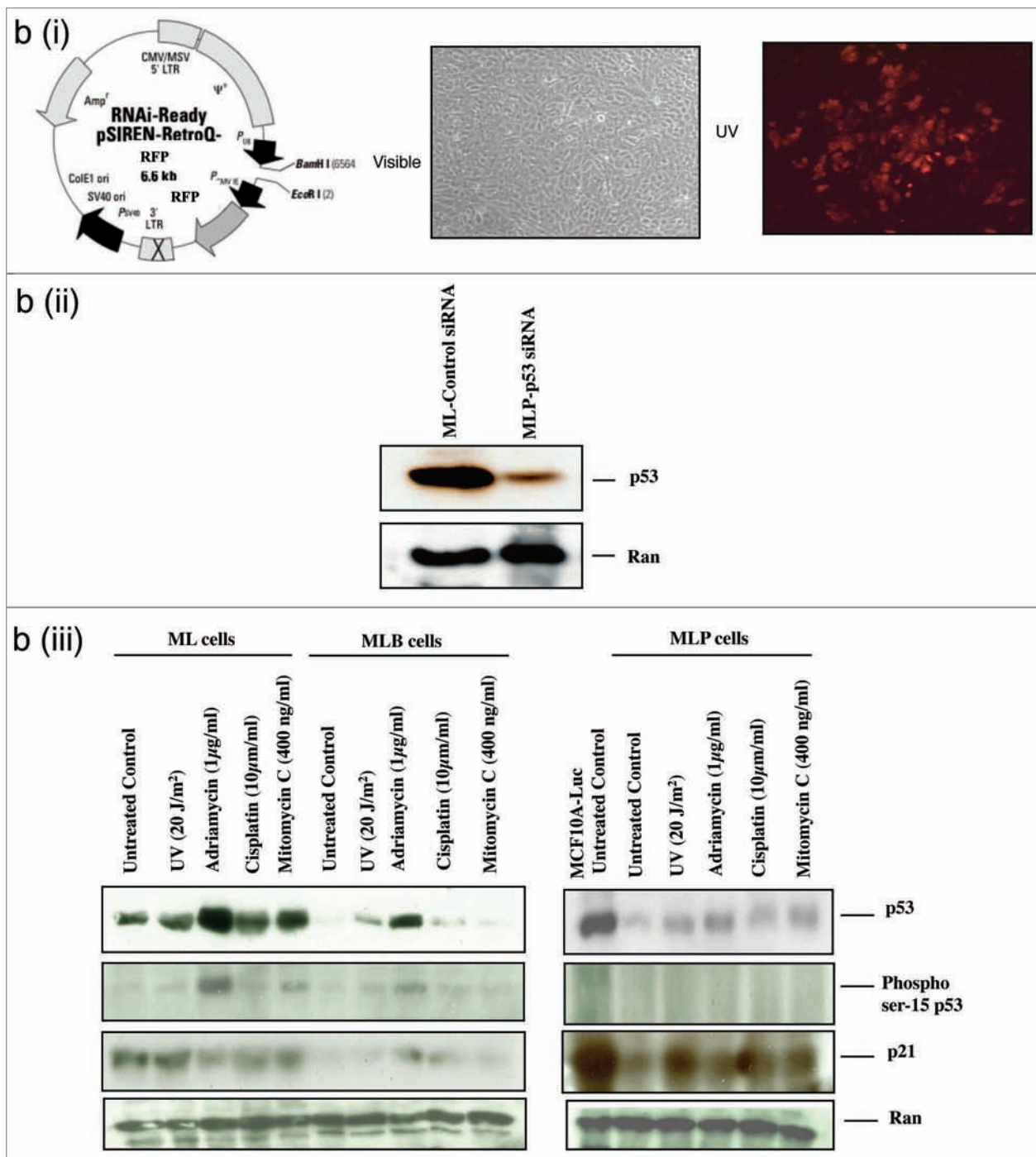


**Figure 1b.** Construction and characterization of p53 stable siRNA knockdown in MCF10A-Luc cells. The retro viral vector map used to clone the annealed double stranded siRNA oligo into BamH I and EcoR I sites. Retro viruses were prepared, target ML and MLB cells were infected as mentioned in materials and methods and sorted for p53 knock down with RFP selection marker by FACS (**Fig 1bi**). Western analysis for evaluating p53 knockdown (**Fig 1bii**), and western analysis for impaired p53 levels, reduced phosphorylation at serine 15 of p53 protein and p21 levels with different DNA damaging agent treatment to show that depletion of BRCA1 can affect the p53 stability. Cells were harvested after 24 hours of different agents treatment except for adriamycin treated cells, collected immediately after 4 hours of treatment (**Fig 1biii**).

natural apoptosis during growth which may have contributed to the increased mass and size of these tumors in vivo.

In addition to growth promoting and apoptotic signals in tumor stroma, another important factor that influences tumor

growth is the tumor vasculature. Blood vessels help not only in supplying oxygen, nutrients, and growth factors to tumor cells but also allow removal of metabolic waste generated by the tumors.<sup>29</sup> A perfect balance between many positive and negative

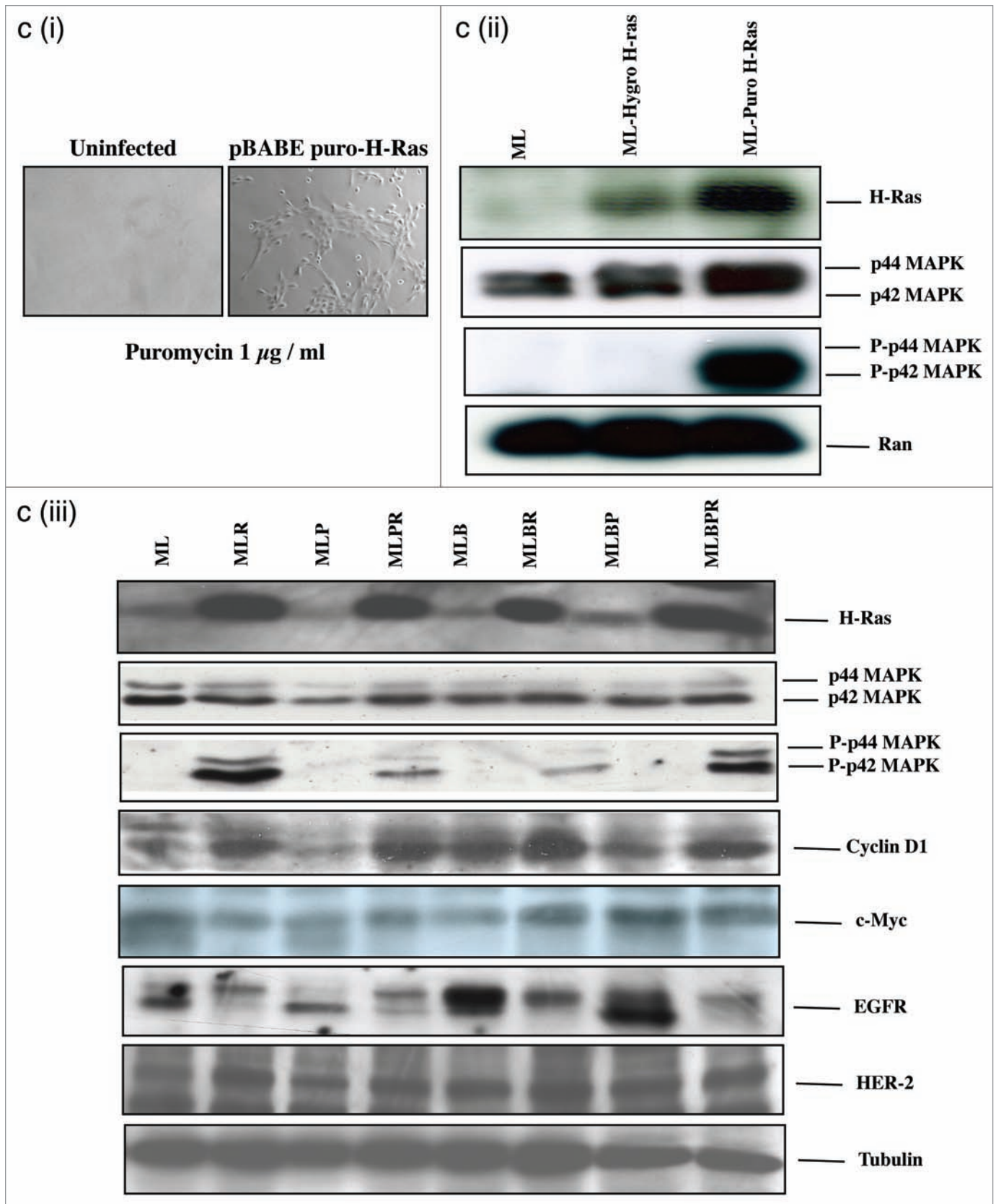


**Figure 1c.** For figure legend, see page 119.

**Figure 1c.** Construction and characterization of different MCF10A-Luc cells stably over-expressing mutant H-Ras. Different target MCF10A-Luc cells were infected with pBABE-Puro H-RasV12 virus and selected for puromycin resistance for three days with a concentration of 1  $\mu\text{g/ml}$  (**Fig 1ci**). Western analysis of H-Ras protein levels and downstream MAPK activity with either pBABE Hygro-Ras or pBABE Puro-Ras transduced cells which were tested to find out the difference in Ras expression levels in a selection marker dependent manner (**Fig 1cii**). Western analysis to identify an increase in different onco protein levels with BRCA1 knockdown (**Fig 1ciii**).

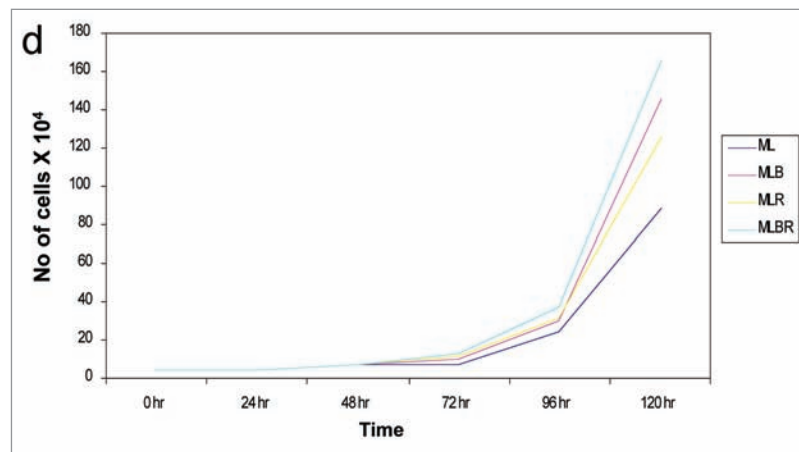


**Figure 1d.** Growth rate of different MCF10A-Luc cells. Different MCF10A-Luc cells were seeded at the density of  $5 \times 10^4$  cells / petri dish, harvested and counted using hemocytometer at different time points as shown. For each time point, average values of triplicates were plotted.

regulators of the neovasculature such as vascular endothelial growth factor (VEGF; angiogenic)<sup>30</sup> and thrombospondin (Tsp-1; anti-angiogenic),<sup>31</sup> determines the angiogenic potential of tumor tissues. The Ras oncoprotein plays a contrasting dual role in being both a stimulator of VEGF expression and an inhibitor of Tsp-1 expression.<sup>32,33</sup> Since our human mammary epithelial cell lines were over-expressed with mutant Ras in combination with depleted levels of tumor suppressor proteins, we therefore tested the levels of both VEGF and Tsp-1 in the different transformed cells and in the corresponding tumor xenografts derived with Ras over-expression. Immunohistochemical analysis of tumor tissues showed a much stronger positive staining for VEGF in tumors lacking BRCA1 as compared to control tumors with normal levels of BRCA1 (**Fig 3ci**). Western blot analysis of those tumor tissues also showed an increase in VEGF protein expression in the BRCA1-deficient tumors (**Fig 3cii, lane 2–3 and 6–7**). Interestingly, the protein level of the anti-angiogenic factor, Tsp-1 was not decreased in transformed cells but was completely lost in tumors derived from those corresponding transformed cells (**Fig 3cii, lane 2–3 and 6–7**). To test whether increased VEGF and decreased Tsp-1 expression in tumor xenografts can result in neovascularisation and enhanced tumorigenicity, tumor sections were stained for CD34 markers.<sup>34–36</sup> CD34 staining showed stronger positive staining in BRCA1-deficient tumors suggesting higher levels of vascularization in that tumor type compared to ones with normal levels of BRCA1 (**Fig 3d**). This enhanced vascularization in BRCA1-deficient tumors may also be partially due to increased VEGF protein levels.

**Epithelial-to-mesenchymal transition (EMT) in Ras-driven mammary tumors.** Many of the natural breast cancer cell lines are metastatic in vivo and establish secondary tumors from

the site of the primary tumor at later stages of cancer progression. Using transformed mammary epithelial cells may be an appropriate model to study the process of breast cancer metastasis as it helps in identifying the molecular changes associated with breast cancer progression. The epithelial-to-mesenchymal transition (EMT) is a process by which epithelial cells undergo many molecular and morphological changes including loss of cell-cell contact, cell polarity, gain of mesenchymal gene expression and mesenchymal-like structural alterations in the cytoskeleton enabling increased motility and invasiveness.<sup>37–40</sup> During the EMT, many known epithelial-specific markers are lost and mesenchymal-specific markers are gained. We were interested in testing the ability of Ras-transformed MCF10A cells used in our experiments to undergo the EMT. Western blot analysis for epithelial-specific markers such as E-cadherin and  $\beta$ -catenin showed loss of expression whereas mesenchymal markers like vimentin and  $\alpha$ -SMA showed a gain of expression (**Fig 4a**). Interestingly, the expression pattern of these markers in Ras-transformed mammary epithelial cells was influenced by its surrounding environment from where the cells were grown. When transformed cells were grown either in the presence of culture medium in vitro or during tumor formation in animals in vivo, E-cadherin expression was lost completely and vimentin expression was enhanced, compared to parental untransformed ML cells (**lanes 1–7 of Fig 4a**). Surprisingly, another epithelial marker expression,  $\beta$ -catenin was diminished in Ras-transformed cells when grown in culture medium but a complete loss of expression was observed only in vivo during tumor formation (**lanes 1–3 with lanes 6 and 7 in Fig 4a**). Another mesenchymal marker,  $\alpha$ -SMA showed increased levels only in tumor tissues in vivo whereas modest expression was only detected in corresponding cells when grown in culture medium in vitro (**lanes**

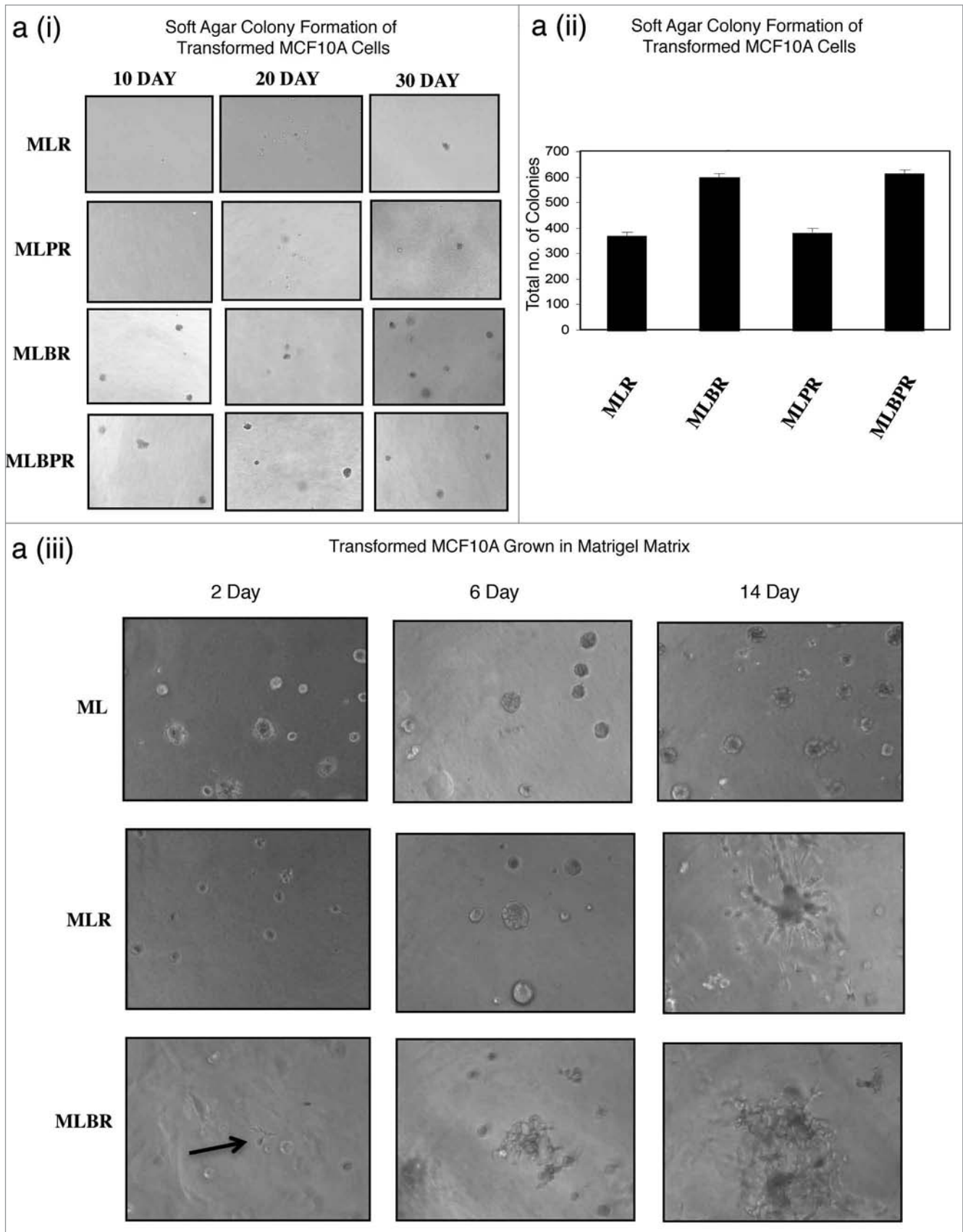


**Figure 2a.** For figure legend, see page 121.

**Figure 2a.** Soft agar, and xenograft growth characteristics of transformed human mammary epithelial cells. 2a. Transformation efficiency of different MCF10A-Luc cells over-expressing mutant H-Ras. Different Ras-transformed cells were seeded on soft agar plates and monitored at regular time intervals. BRCA1-depleted Ras-transformed (MLBR & MLBPR) cells formed visible growth colonies as early as the tenth day and showed a higher increase in total number by thirty days of growth. Average values of total colonies from triplicate plates were counted and plotted (**Fig 2ai and Fig 2aii**). Matrigel matrix growth assay was done to identify abnormalities in acinar structures with Ras overexpression. As early as on second day, MLBR cells showed highly irregular lobular structures different from control ML cells which formed a uniform monolayer spherical structure with luminal epithelial cells surrounding a hollow lumen (**Fig 2aiii**).

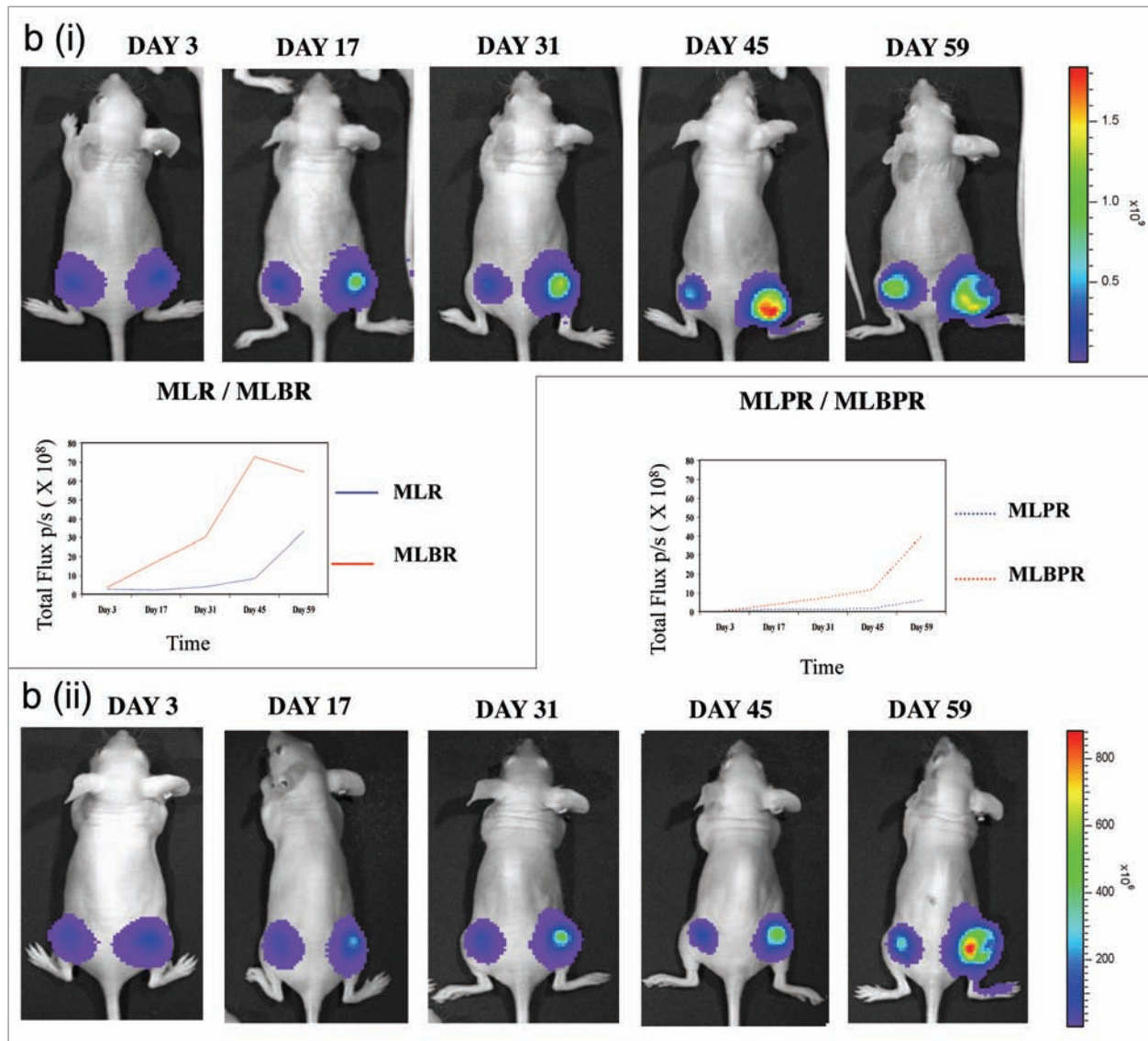


**Figure 2b.** For figure legend see p.122.

1-3 with lanes 6 and 7 in Fig 4a). These results suggest that the tumor microenvironment consisting of matrigel matrix can influence the gene expression pattern of transformed cells to promote tumorigenesis and metastasis in vivo, much different from the gene expression pattern of the same cells grown in culture medium. Unexpectedly, depletion of both BRCA1 and p53 protein levels together in ML cells also resulted in complete loss of epithelial marker expression E-cadherin indicating that loss of these two major tumor suppressors may contribute to structural alterations in mammary epithelial cells that

can promote migratory properties of transformed cells during advancement of breast cancer (lane 11 in Fig 4a). Using the same antibodies specific for epithelial and mesenchymal markers in further immunocytochemical and histochemical analysis with either these Ras-transformed mammary epithelial cells or their corresponding tumor xenografts derived in vivo respectively, confirmed the process of EMT (Fig 4b–4d). As observed in western blot analysis (Fig 4a), immunocytochemical analysis also confirmed the complete loss of E-cadherin and partial loss of  $\beta$ -catenin expression with Ras overexpression

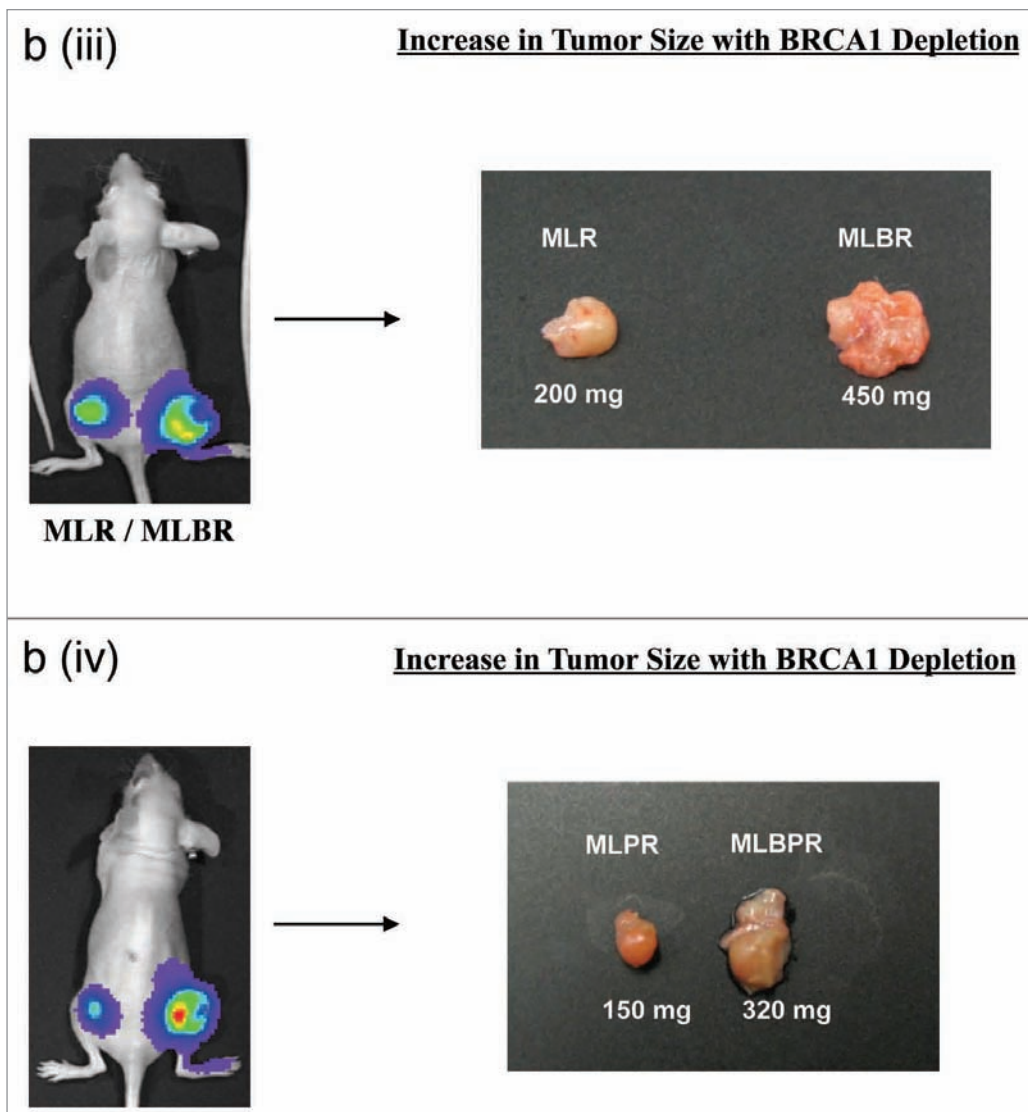


**Figure 2b.** Aggressive tumor formation of BRCA1-depleted MCF10A-Luc cells over-expressing mutant H-Ras. A group of ten animals for each transformed cell line was implanted subcutaneously on the flank region.  $10 \times 10^6$  cells/injection was used. In each individual animal, the left side was injected with tumor cells having normal levels of BRCA1 and the right side was injected with tumor cells having depleted levels of BRCA1 (**combination of MLR / MLBR cells as in Fig 2bi or MLPR/MLBPR cells as in Fig 2bii**). Animals were imaged periodically every week and the average signal intensities from growing tumors were calculated and plotted. 50% of the animals formed tumors with such subcutaneous injections in flanks (**Table I**). After nearly 2 months, animals were sacrificed, tumors were harvested, sizes measured and processed for further histological analysis. BRCA1 deficient MCF10A tumors were much aggressive and bigger in size than tumors with normal levels of BRCA1, and p53 depletion did not enhance in vivo tumorigenicity (**Fig 2biii and Fig 2biv**).

(Fig 4b). Similarly, intense staining was detected only for vimentin expression in transformed cells by immunocytochemical analysis (Fig 4c) and a stronger signal was observed for  $\alpha$ -SMA expression in tumor xenografts with immunohistochemical analysis (Fig 4d). All these results suggested the occurrence of EMT in Ras-transformed MCF10A cells. To confirm the migratory properties of these transformed cells, a transwell migration assay using serum as chemo-attractant was performed in vitro. Interestingly, depletion of BRCA1 enhanced the migratory properties of transformed cells with an increase in the total number of migrating cells, even in the absence of chemo-attractant serum (Fig 4e). In vivo bio-imaging of animals bearing MLBR tumors

with injection of MMP680 fluorescent probe specific for detecting matrix metalloproteases (MMPs) also indicated the ability of these tumors to invade the neighboring tissues with secretion of MMPs (Fig 4f). When these Ras-transformed, BRCA1-depleted mammary epithelial (MLBR) cells were implanted into mammary fat pads of nude mice, they also showed metastasis to different internal organs such as lymph nodes and liver after 60 days of implanting cells (Fig 4gi and 4gii). Hematoxylin and Eosin staining of lymph node tissue sections from tumor-bearing animals showed much larger cells with more cytoplasm and strong  $\alpha$ -green signal under uv light in microscopy confirming the metastasis of tumor cells from their original site of

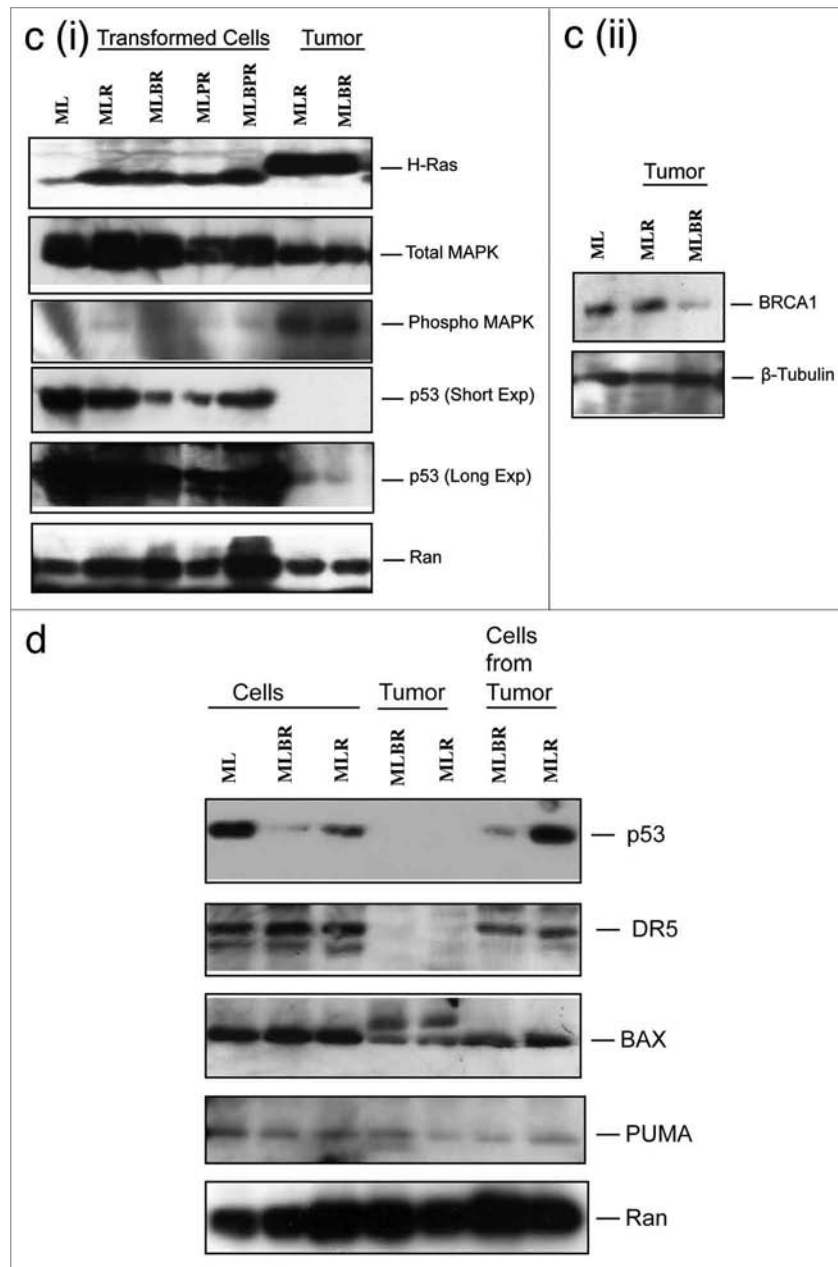


**Figure 2c and d.** (2c) Western blot analysis of Ras-transformed MCF10A-Luc tumor xenografts. Western analysis for protein lysates prepared from harvested tumor xenografts was done to look for the levels of H-Ras, MAPK activity, p53 and BRCA1 (**Fig 2ci and Fig 2cii**). p53 expression was greatly reduced only in tumor xenografts but not in corresponding cells grown in petri dish. (2d) Western blot analysis of levels of p53 and its pro-apoptotic downstream targets in Ras-transformed MCF10A-Luc tumor xenografts. Different downstream pro-apoptotic targets of p53 such as DR5, BAX, PUMA were tested in transformed tumor cells, in corresponding tumor xenografts and in cell lines re-established from tumor tissues. Expression levels of p53 and DR5 were greatly reduced only in tumors.

implantation in the mammary fat pads (**Fig 4h**). During such fat pad implantations, only BRCA1-depleted Ras-transformed (MLBR) cells were able to grow and establish tumors in nude animals whereas MLR tumors with normal levels of BRCA1 failed to form tumors in mammary fat pads (**Table 1, complete data not shown**).

**Genomic instability and sensitivity towards DNA-damaging agent treatment.** Our results indicate that deficiency of BRCA1 in MCF10A cells with stable knockdown can cause

multiple centrosomes that can eventually result in unequal segregation of chromosomes during mitosis and loss of genomic balance in resultant daughter cells (**Fig 1aiv**).<sup>14</sup> During mitosis, the chromosomes of BRCA1-deficient cells are highly coiled and decondensed in architecture indicative of a susceptibility to chromatid breaks and unwanted chromatid exchanges in the form of recombination events (**Fig 1aiii**).<sup>24,41</sup> Apart from being a classical tumor suppressor in breast and ovarian tissues, another major function of BRCA1 is, its universal role in safeguarding

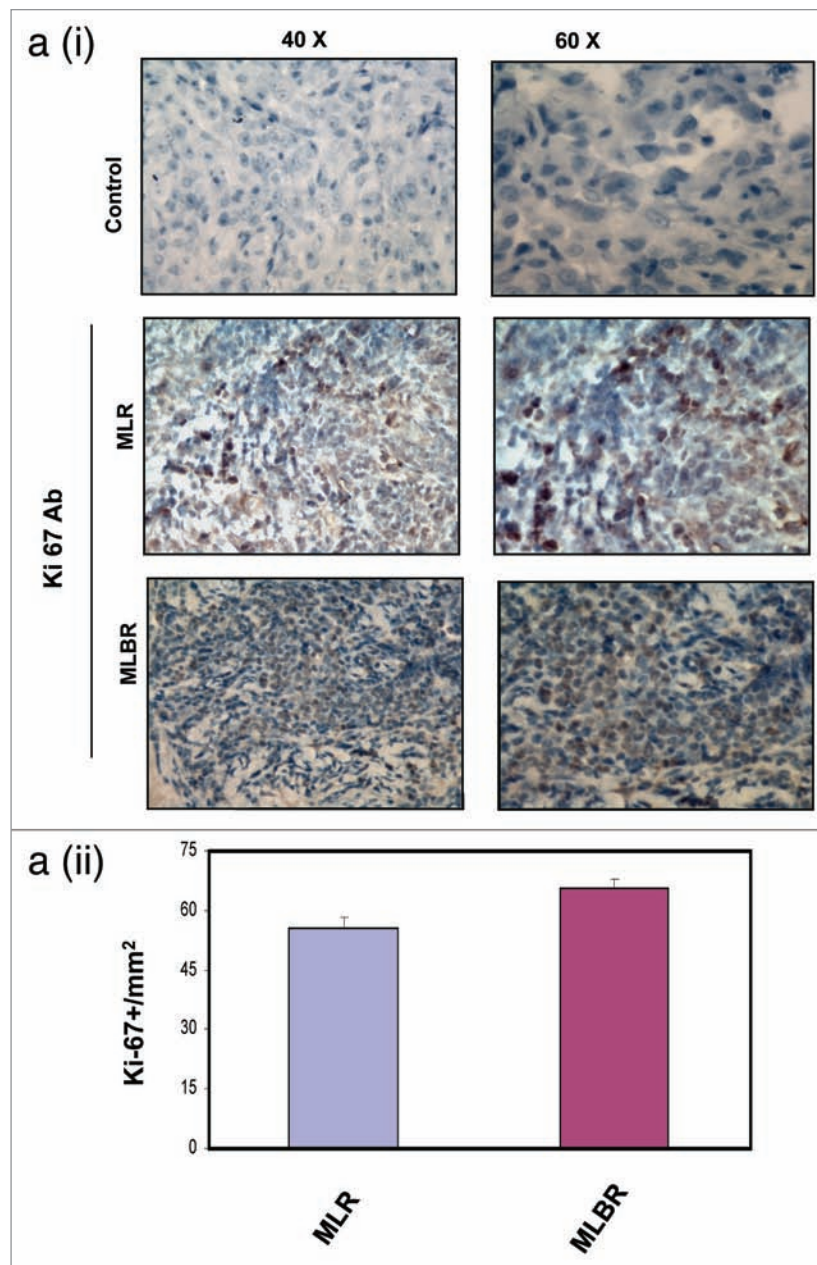


**Figure 3a.** Proliferation, apoptosis, and angiogenesis effects of tumor suppressor BRCA1 knockdown and H-Ras-mediated transformation of human mammary epithelial cells. (3a) Immunohistochemical staining of tumor xenografts with Ki-67 antibody for proliferation. Histological staining was done using Ki-67 antibody to look for the proliferation in both MLR and MLBR tumor tissues (**Fig 3ai**) and quantification of average values from three such independent staining was plotted (**Fig 3aii**).

the genome. BRCA1 also acts as sensor or transducer of the DNA damage signal by recruiting other DNA repair proteins.<sup>42</sup> During the early stages of DNA damage, ATM gets activated by auto-phosphorylation and phosphorylates downstream target proteins including Chk2 and H2AX.<sup>43</sup> It has been reported that Ras-mediated mammary epithelial cell transformation can be accompanied by diverse genomic rearrangements.<sup>7</sup> Thus, we tested what happens to DNA damage signaling pathways in MLR and MLBR cells, with respect to activation (phosphorylation) of ATM and H2AX. Unexpectedly, both MLR and MLBR cells showed activation of ATM (phospho ser-1981), and H2AX

( $\gamma$ -H2AX) even in the absence of any DNA damaging agent treatment (**Fig 5a**). BRCA1 deficiency also resulted in enhanced sensitivity towards DNA cross-linking agents like mitomycin-c and  $\gamma$ -irradiation.<sup>12,44</sup> Treating these Ras-transformed mammary epithelial cells with another DNA-damage inducing agent, adriamycin (0.25  $\mu$ g/ml) resulted in two different results when either BRCA1 alone is depleted or together with p53. Compared to control ML cells, over-expression of Ras in ML cells resulted in chemoresistance at 48 hr. Interestingly, BRCA1-deficient MLBR cells showed much higher sensitivity as compared to ML and MLR cells, at 48 hr. But, double-depletion of both BRCA1

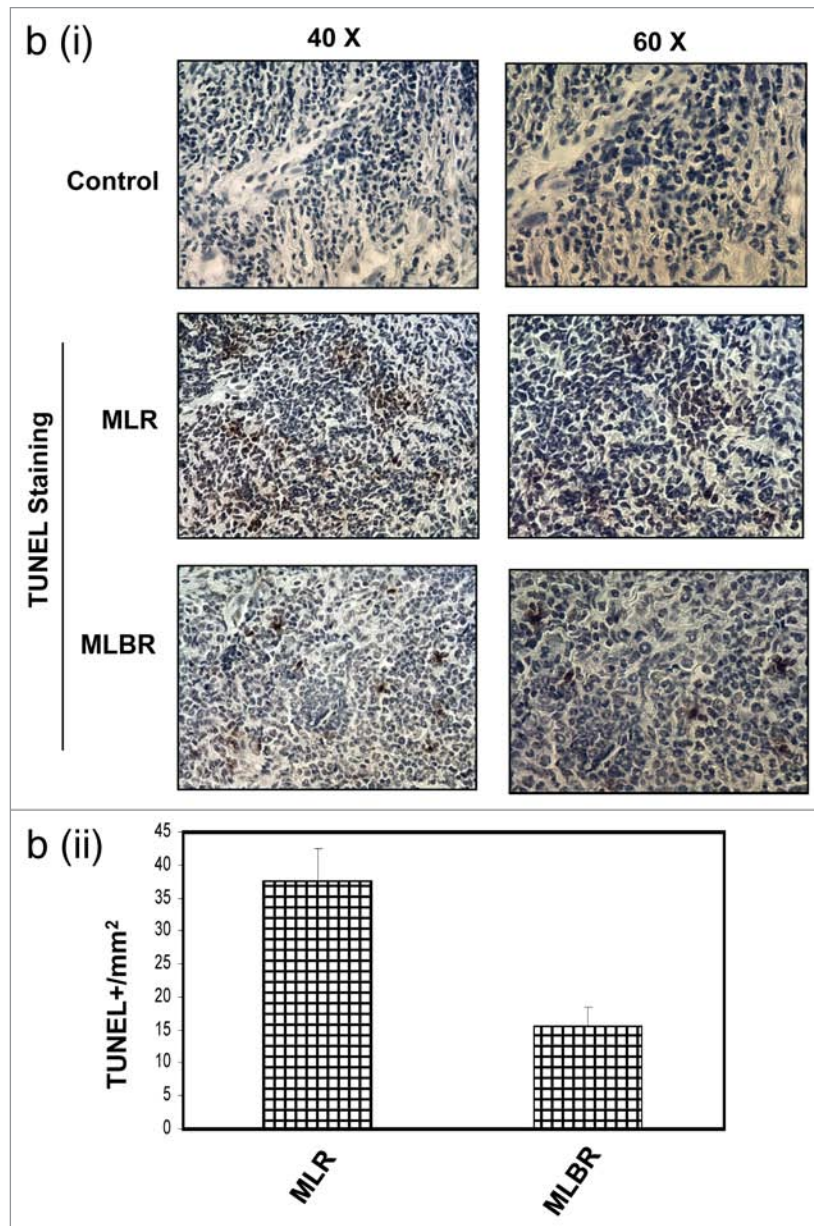


**Figure 3b.** TUNEL staining of tumor xenografts for apoptosis. TUNEL staining was done to look for apoptotic cells in both MLR and MLBR tumor tissues (**Fig 3bi**) and quantification of average values from three such independent staining was plotted (**Fig 3bii**).

and p53 in MLBPR cells showed reduction in BRCA1-mediated sensitivity towards adriamycin treatment at the same time point (**Fig 5b**). These results suggest that BRCA1 and p53 proteins may have different functions in mediating cellular responses to adriamycin treatment.

### Discussion

Using retroviral-mediated shRNA expression system, we show that successful establishment of a viable human mammary epithelial cell line deficient for two major tumor suppressors of breast epithelium-BRCA1 and p53. Stable knock down of BRCA1 alone in MCF10A cells (MLBR) affects many different biological

functions such as centrosomal duplication, chromosomal condensation during mitosis, etc. due to the lack of ubiquitin ligase activity on many diverse substrates like  $\gamma$ -tubulin and topoisomerase II- $\alpha$ , respectively (**Fig 1aiii and 1aiv**). Interestingly, depletion of BRCA1 also causes impaired p53 stability in human mammary epithelial cells through an unknown mechanism (**Fig 1biii**), consistent with a previous report from our laboratory that BRCA1 over-expression can stabilize the p53 protein.<sup>15</sup> MLB cells also behave in a very similar manner to breast tumors from the *Brcal*-conditional knockout mouse, in showing elevated levels of different oncoproteins such as cyclin D1, c-myc, Her-2 and EGFR<sup>17</sup> suggesting this genetically engineered human cell line can very well mimic the biology of BRCA1-deficient

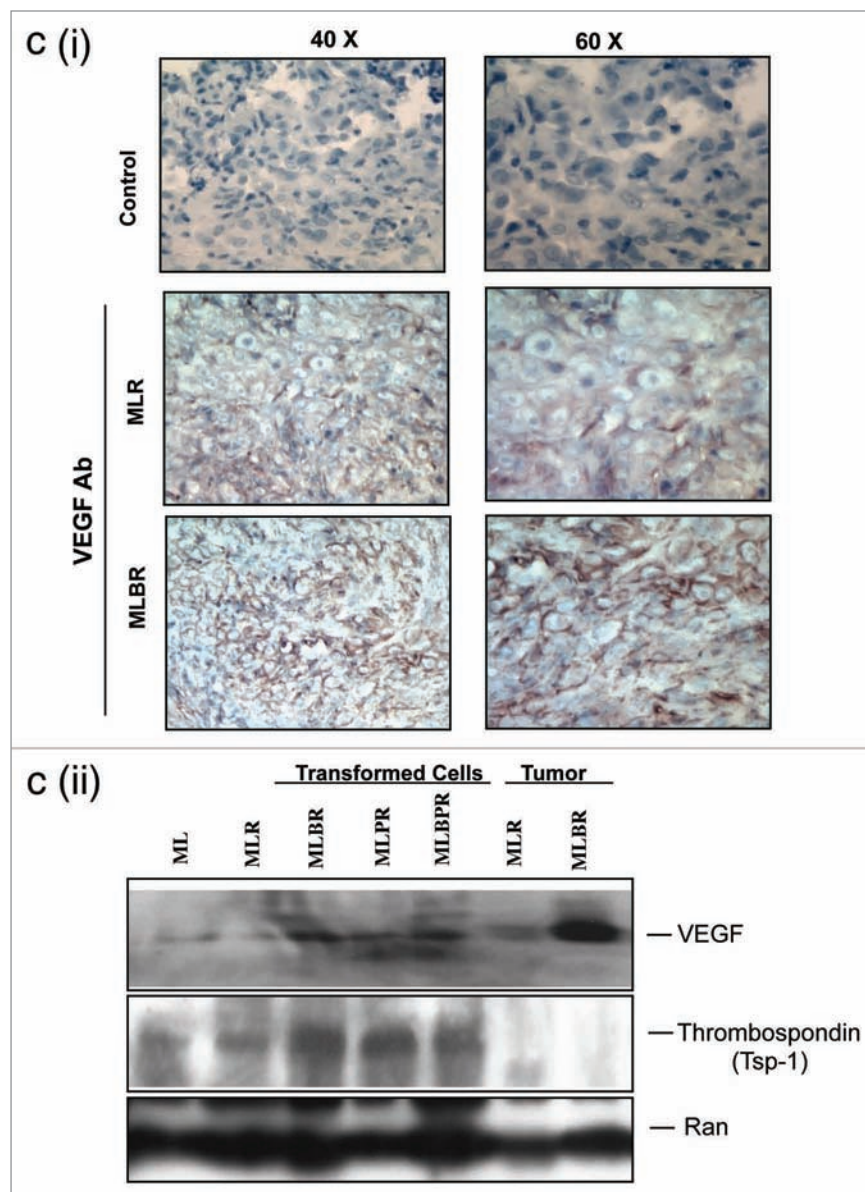


**Figure 3c.** Immunohistochemical staining and western blot analysis of tumor xenografts for VEGF. Histochemical staining was done using VEGF antibody in both MLR and MLBR tumor xenografts (**Fig 3ci**). Immuno blot analysis was done to check the levels of pro-angiogenic—VEGF and anti-angiogenic—Thrombospondin (TSP-1) in different Ras-transformed cells and in MLR & MLBR tumors showing BRCA1 depletion leading to higher VEGF levels and lesser thrombospondin in tumors compared to its corresponding transformed cells (**Fig 3cii**).

tumors of known conditional knockout animal models and thus making it a simplified tool to study the functions of BRCA1 in human breast tumorigenesis (**Fig 1ciii**). As reported by Elenbaas et al.,<sup>7</sup> we also observed a failure of successful transformation of MCF10A cells with lesser levels of H-Ras protein when hygromycin marker was used to select for pBABE-H-RasV12 transduced cells (complete data not shown). At present, the molecular mechanism of selection marker driving the stronger expression levels of H-RasV12 in pBABE vector, still remains unclear.

Unlike in breast cancer patients who carry mutations in Brcal and p53 genes, depletion of both BRCA1 and p53 either alone or together is not sufficient to transform a normal mammary epithelial cell into a cancer cell in vitro. Our in vitro model

system suggests that for efficient transformation of human breast epithelium, apart from blocking BRCA1 and p53 tumor suppressor pathways in breast epithelium, additional event such as oncogenic activation is also important to promote tumorigenesis.<sup>7</sup> Absence of functional BRCA1 and p53 has been shown to increase genomic instability and hypersensitivity towards gamma-irradiation in Brcal-conditional knockout mouse models.<sup>12</sup> Enhanced genomic instability may result in accumulation of additional mutations in oncogenes randomly over a period of time, resulting in oncogenes activation and accelerated growth of those cells bearing such activated mutant oncogenes. Our results from both in vitro and in vivo experiments support the hypothesis that loss of functions of both BRCA1 and p53 in

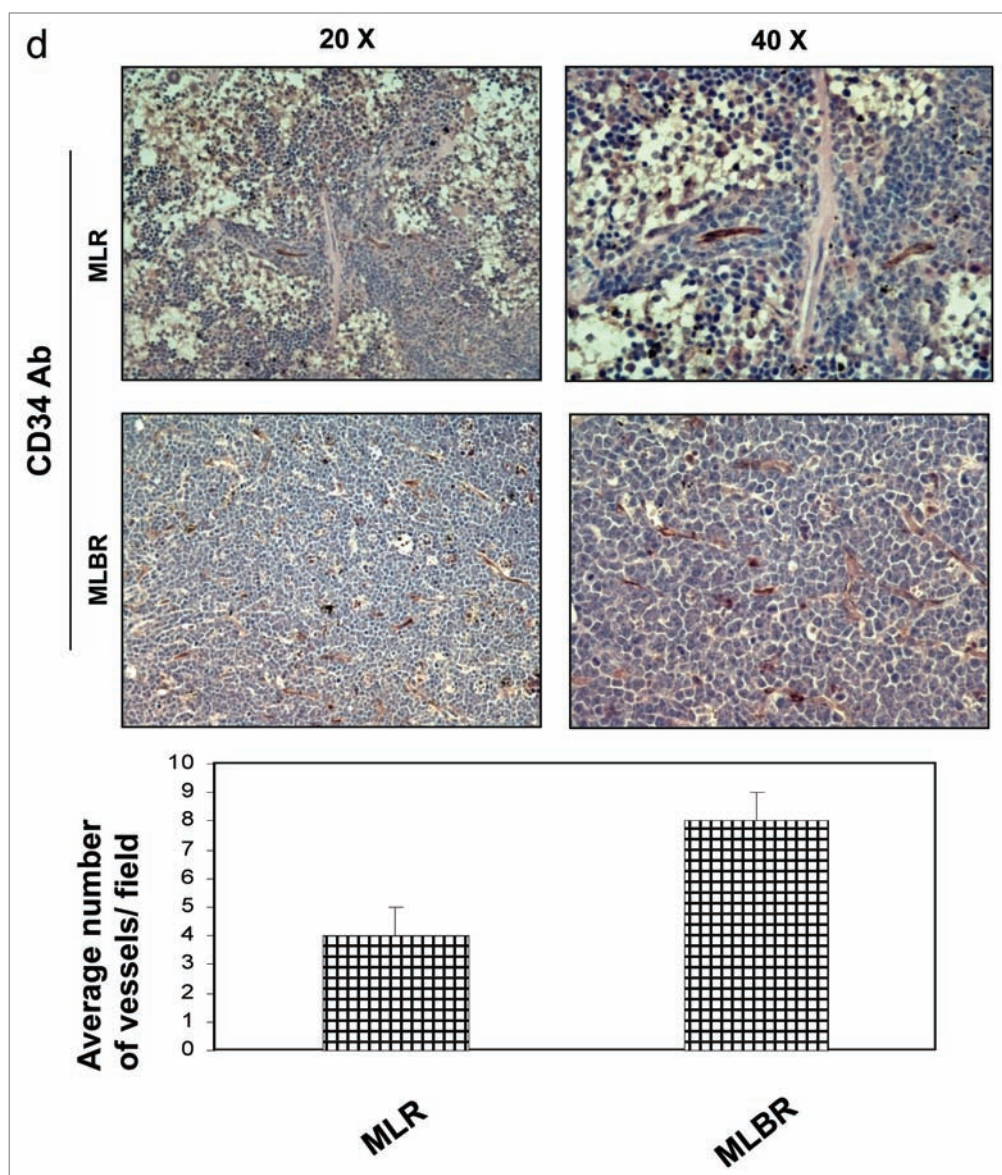


**Figure 3d.** Immunohistochemical staining of tumor xenografts for CD34. Histochemical staining was done in MLR and MLBR tumor xenografts using CD34 antibody to look for neovascularisation and quantification of such positive staining from three independent experiments (**Fig 3d**) showing BRCA1 depleted tumors were more vascularised.

human breast epithelium must also be accompanied by a gain of function in the form of an oncogene activation to convert effectively a normal mammary epithelial cell into a cancer cell. Depletion of BRCA1 and p53 either alone or together without over-expression of H-RasV12 neither formed soft agar colonies nor tumors in animals (data not shown). But, both soft agar colony formation assays and in vivo tumor formation in mouse models showed a significant enhancement of the total number of soft agar colonies and highly aggressive, larger sized tumors only when BRCA1 depletion was combined with H-Ras over-expression (**Fig 2a and 2b**). Interestingly, even without any p53- or BRCA1-specific shRNA expression, the p53 protein level was reduced in tumor xenografts for unknown reasons. Reduced p53 expression in tumor tissues was reflected in reduced levels of its

pro-apoptotic downstream targets like DR5 and BAX (**Fig 2d**). Additional depletion of p53 by gene knockdown, either alone or in combination with BRCA1 did not enhance the tumorigenicity of Ras-transformed MCF10A cells both in vitro and in vivo. In matrigel matrix growth, BRCA1-deficient Ras-transformed MCF10A-Luc (MLBR) cells showed structural alterations by as early as the second day indicating these cells may acquire better adaptability to grow and establish tumors more quickly in vivo within the matrigel matrix micro environment (**Fig 2aiii**). All these results suggest that BRCA1 may play a more important role in tumor suppression in human breast epithelium.

A balance between proliferation and apoptosis may determine the size of a growing tumor. In our experimental models, analysis with Ki-67 specific antibody revealed the proliferation rate

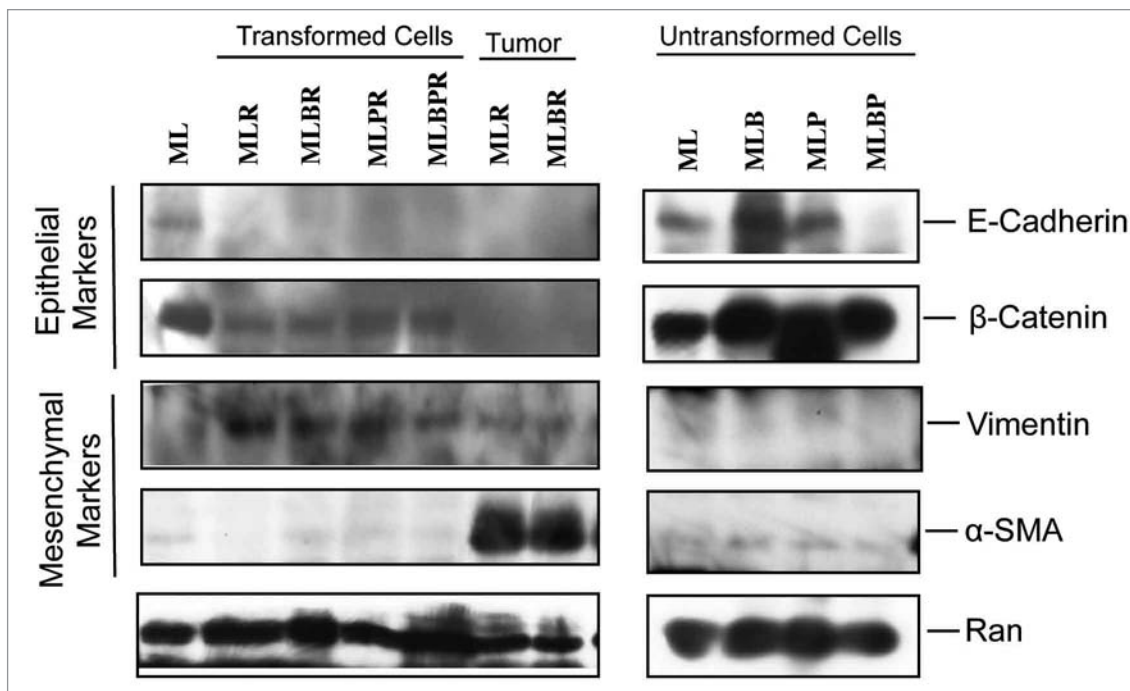


**Figure 4a.** Western analysis of EMT markers in Ras-transformed MCF10A-Luc tumor xenografts. Immuno blot analysis using antibodies specific for both epithelial markers like E-cadherin,  $\beta$ -catenin and mesenchymal markers like vimentin and  $\alpha$ -SMA confirmed the occurrence of epithelial to mesenchymal transition.

was nearly the same in both BRCA1-depleted Ras-transformed xenograft tumors (MLBR) and tumors with wild-type levels of BRCA1 (MLR). However, TUNEL-staining confirmed a different rate of apoptosis in these two tumors suggesting that BRCA1-deficiency leads to reduced apoptotic rate in a growing tumor which is a major cause contributing to larger tumor size in vivo (Fig 3a and 3b). In other words, BRCA1 may be essential for controlling apoptosis during normal mammary tissue development, the absence of which can result in lack of programmed cell death and an increase in total cell number. Another major factor that can influence the size of a growing tumor in vivo is, neovascularisation. The link between vascular endothelial growth factor, VEGF and new blood vessel formation in a growing tumor has been very well studied.<sup>29,30, 32,33</sup> It has also been documented how BRCA1 can negatively regulate the levels of VEGF in ER positive cells through estrogen receptor alpha—ER $\alpha$ .<sup>45,46</sup> In our xenograft tumor models, we show BRCA1-depletion can lead to an increase in VEGF levels in Ras-transformed MCF10A tumors in an estrogen receptor  $\alpha$  independent manner as MCF10A is an ER negative cell line (Fig 3c). So, this cell line may help shed new light in identifying the mechanism of VEGF regulation by BRCA1 in estrogen receptor-negative cell lines. It is also possible that VEGF regulation may be influenced by HIF-1 in a hypoxic tumor environment. Increased pro-angiogenic factor VEGF and decreased anti-angiogenic factor Thrombospondin (Tsp-1) may well contribute to new blood vessel development in expanding tumors. Our experimental models show that both tumors with either normal levels of BRCA1 or depleted levels, show lack of Tsp-1 expression compared to their corresponding transformed

cells grown in vitro, whereas more than a three-fold increase in VEGF levels is observed in tumors lacking BRCA1 (MLBR) as compared to tumors with normal levels of BRCA1 (MLR). This suggests that apart from reduced apoptosis in tumors, BRCA1-deficiency may also provide further growth advantage to the developing tumor by recruiting more endothelial cells that will reflect in higher levels of new vascularization. CD34 staining of tumor xenografts for endothelial cell recruitment confirmed that indeed BRCA1-deficient tumors have higher levels of blood vessel formation that also facilitates an aggressive tumor growth compared to lesser vascularization in tumors with normal levels of BRCA1 (Fig 3c). This observation may have potential clinical application as anti-angiogenic drugs can be used to treat breast cancer patients effectively who have BRCA1 mutations.

Our results using both in vitro and in vivo approaches, strongly indicate that H-Ras over-expression not only transforms the MCF10A cells but also makes the cell undergo the epithelial-to-mesenchymal transition leading to loss of epithelial-specific markers, appearance of mesenchymal markers and secretion of MMPs, collectively all contributing to many new characteristics including cytoskeleton structural alterations, and increased motility and invasiveness. In vivo studies in nude animals showed enlargement of the spleen when cells were implanted subcutaneously in the flank region though we failed to detect any metastatic secondary tumors in internal organs of animals by in vivo imaging approaches to trace the marker gene expressions such as Luciferase or ZS-Green (data not shown). But, when cells were implanted in the mammary fat pads of animals, metastasis was detected mainly in lymph nodes and

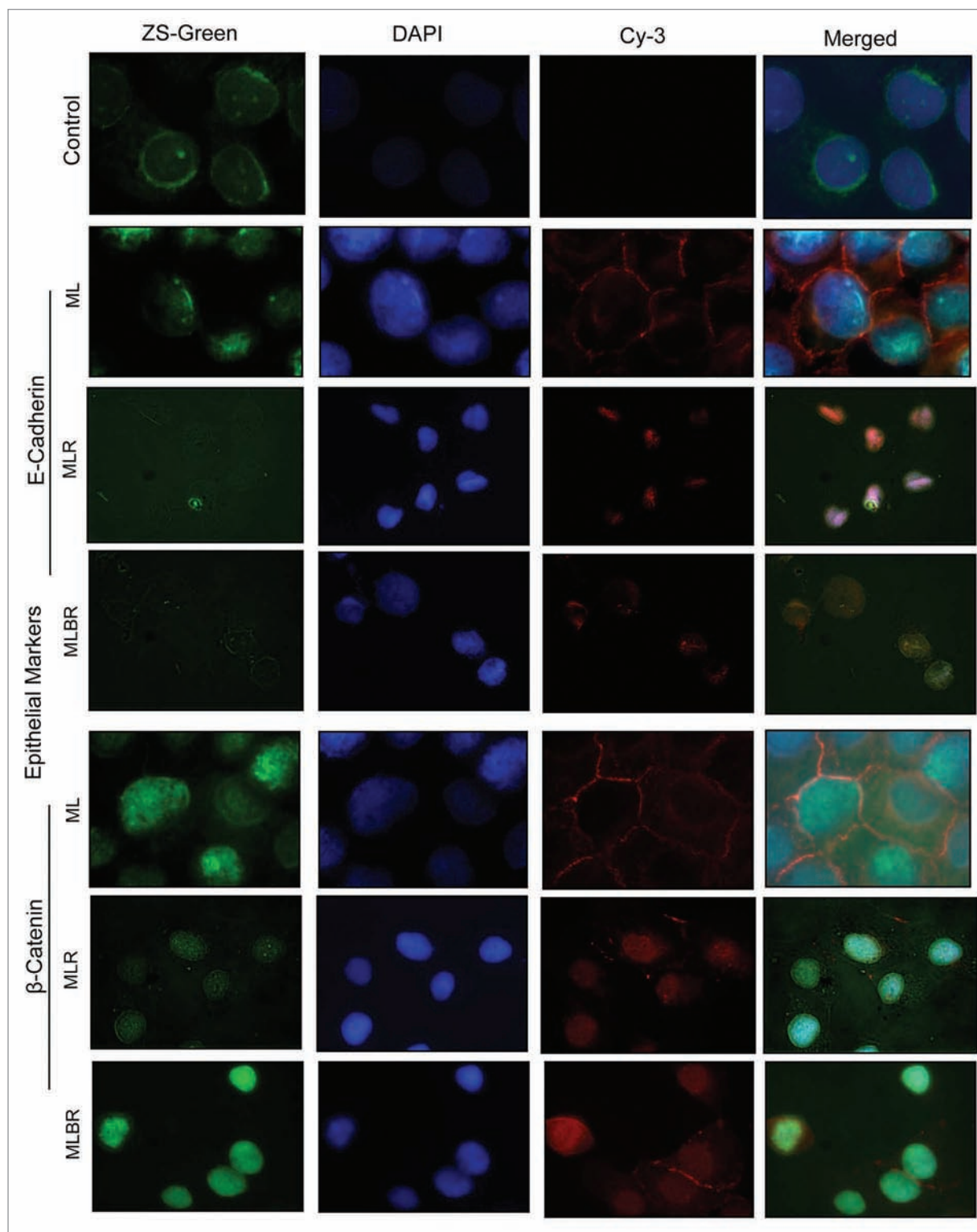


**Figure 4b.** Epithelial marker-specific staining of Ras-transformed MCF10A-Luc cells. Immuno cytochemical staining of transformed MCF10A-Luc cells with antibodies specific for epithelial markers, showing the loss of E-cadherin and  $\beta$ -catenin expression.

liver by imaging approaches (Fig 4g and Fig 4h). Interestingly, only MLBR cells were able to form tumors in mammary fat pads whereas MLR cells with normal levels of BRCA1, failed to establish tumors in the mammary fat pads of animals. This

may partially be due to the ability of BRCA1-deficient cells to adapt faster to their natural surroundings i.e. in the mammary fat pads or to interact within the tumor microenvironment containing matrigel matrix as evidenced in matrigel growth assay

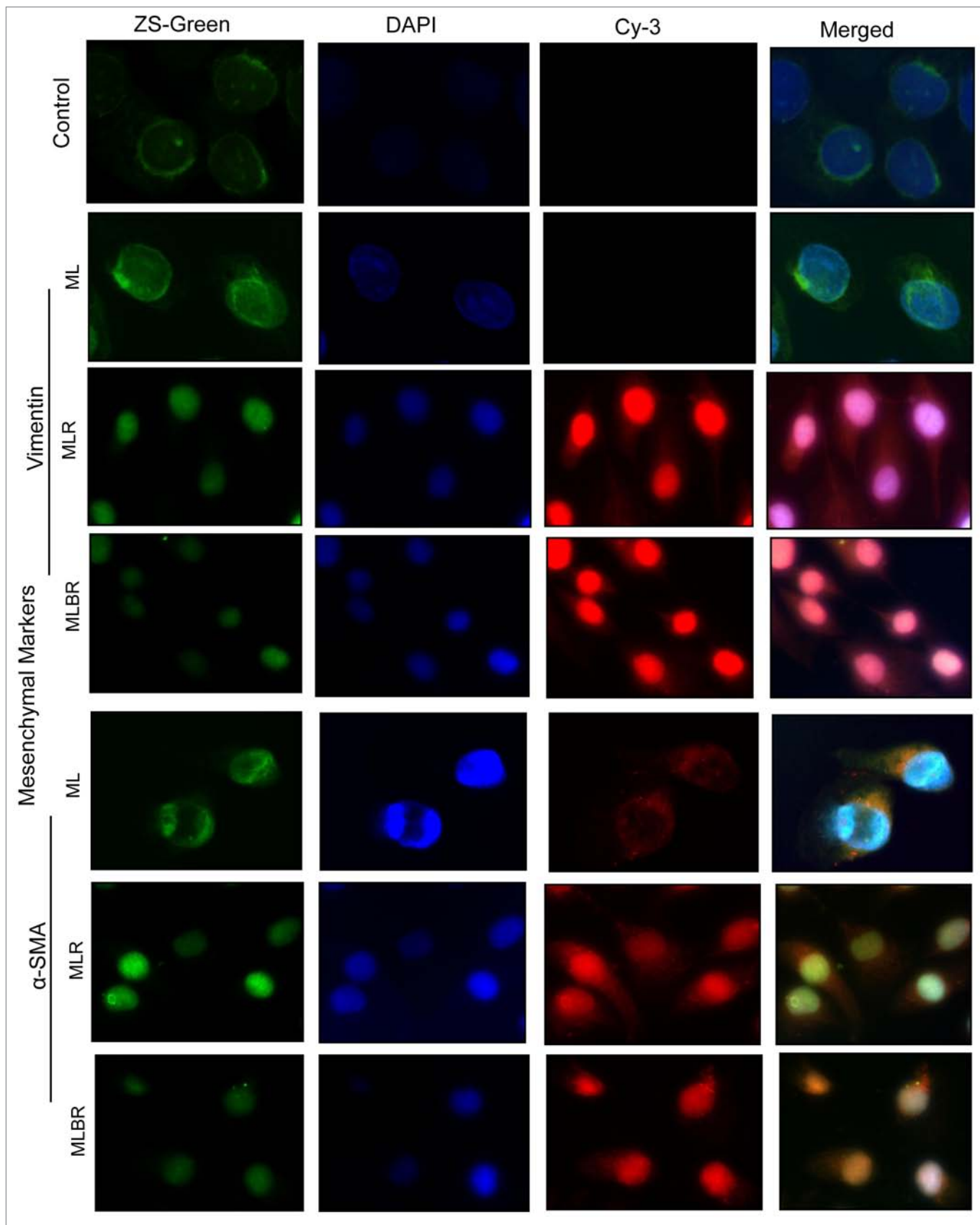


**Figure 4c.** Mesenchymal marker-specific staining of Ras-transformed MCF10A-Luc cells. Immuno cytochemical staining of transformed MCF10A-Luc cells with antibodies specific for mesenchymal markers, showing the appearance of vimentin and  $\alpha$ -SMA expression.

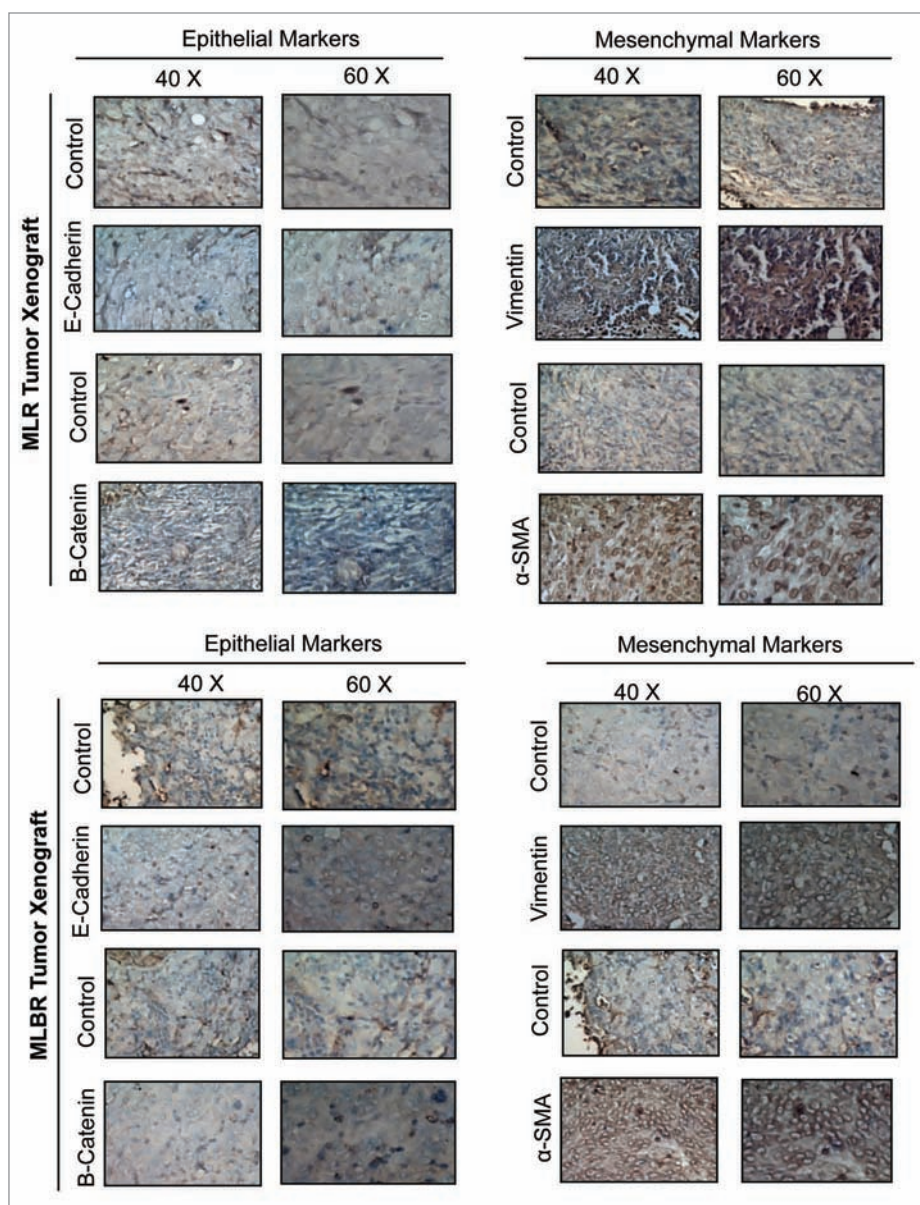


**Figure 4d.** Epithelial-mesenchymal transition in Ras-transformed MCF10A-Luc tumor xenografts. Immunohistochemical analysis using antibodies specific for both epithelial markers like E-cadherin,  $\beta$ -catenin and mesenchymal markers like vimentin and  $\alpha$ -SMA confirmed the occurrence of epithelial to mesenchymal transition in tumor xenografts.

(Fig 2a<sub>iii</sub>). There are many known factors which can promote EMT and breast metastasis such as Twist,<sup>47</sup> Goosecoid,<sup>48</sup> Snail,<sup>49-51</sup> Slug,<sup>52,53</sup> SIP1,<sup>54</sup> FOXC2<sup>55</sup> and different microRNAs like miR-10b,<sup>56</sup> miR-373 and miR-520c.<sup>57</sup> As our result from in vitro migration assay and in vivo lymph node metastasis suggest that MLBR cells have higher migratory capacity (Fig 4d, 4g and 4h), it is tempting to speculate that BRCA1 may be acting as suppressor and may be involved in down-regulation of any of these known metastatic promoting genes. It will be interesting to test in the future whether these known factors can be down-regulated in a BRCA1-dependent manner in breast epithelium using these transformed mammary epithelial cells with stable BRCA1 knockdown.

Among the multiple functions of BRCA1, maintaining genomic stability is very crucial as witnessed in many patients, where BRCA1 mutations are also associated with secondary mutations in other tumor suppressor genes such as p53, or PTEN. Additional mutations may occur randomly in the genome in the absence of a functional BRCA1 as these cells are deficient in DNA repair pathways.<sup>58-60</sup> It has been reported that the genome of transformed human mammary epithelial cells with over-expression of h-TERT, SV40 large T-Antigen and H-Ras can have multiple genetic changes.<sup>7</sup> Interestingly in our model system, the Ras-transformed mammary epithelial cells showed activation of both ATM and H2AX even in the absence of DNA-damaging agent treatment suggesting these cells may harbor either irreparable

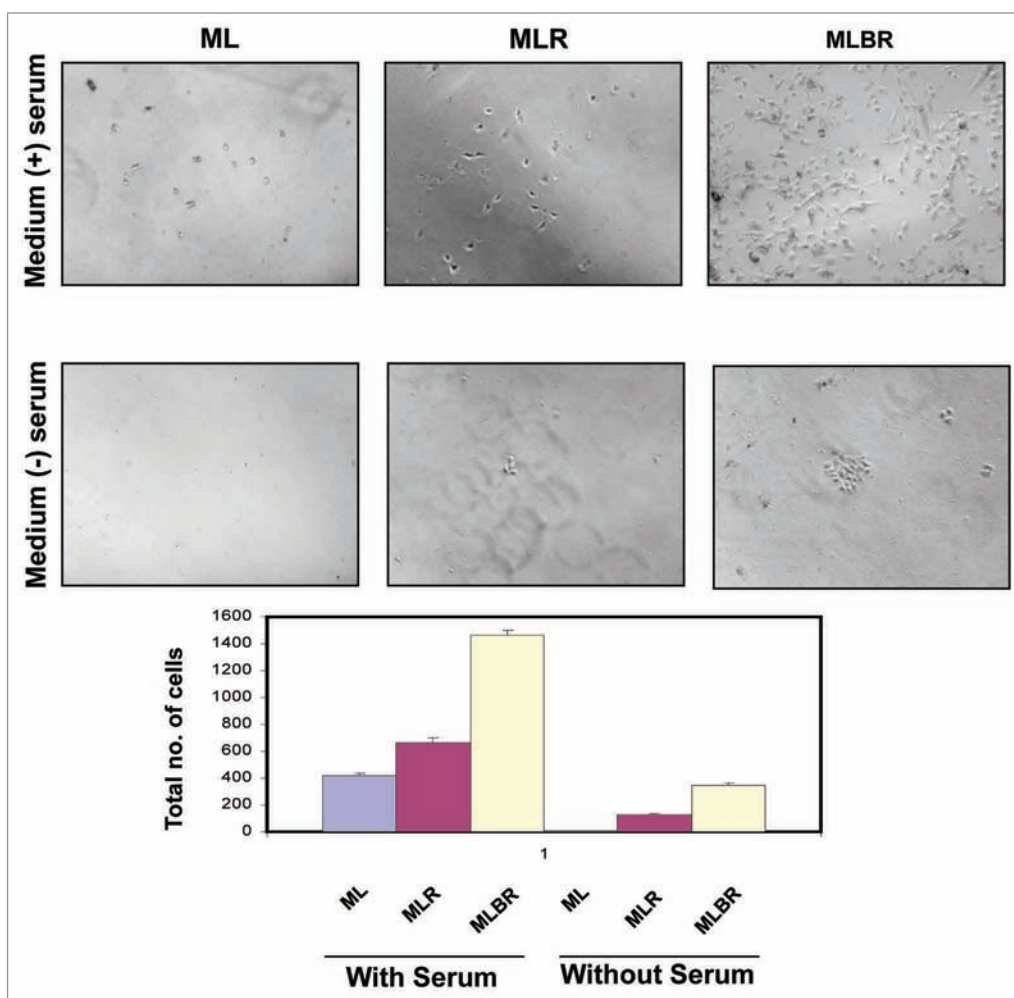


**Figure 4e.** Transwell migration assay for Ras-transformed MCF10A-Luc cells. Transformed cells showed higher migratory property from top well to bottom well with BRCA1 depletion whereas control cells failed to show any migration in the absence of chemo-attractant serum at bottom well. Cells were seeded at top well, incubated for 4 days at 37°C. Average value of total number of cells showing migration was counted from triplicate wells and plotted.

DNA damage due to higher levels of genomic instability or defective DNA repair signaling pathways (Fig 5a). BRCA1 depletion in the same genetic background, further elevates the total number of cells harboring such a defective genome. These cell lines may provide a tool to identify the genomic loci that are selectively undergoing genetic changes in a BRCA1-dependent manner, if any.

Though both p53 and BRCA1 are guardians of the genome, absence of each protein can have different effects on outcome to therapeutic responses. Our results with adriamycin treatment of transformed cells indicate that over-expression of H-Ras can provide chemoresistance to transformed breast cancer cells against adriamycin-mediated DNA damage whereas depletion of BRCA1 can overcome this H-Ras mediated resistance and make the cells more sensitive towards adriamycin treatment. Double depletion of both p53 and BRCA1 can make breast cancer cells chemoresistant against adriamycin treatment, suggesting different functions of these two tumor suppressors in response to

therapeutic treatment (Fig 5b). This approach can be exploited in further studies, by specifically blocking the BRCA1 pathways and making cells more responsive to chemotherapeutic treatments.

In summary, we have created a stable knock-down mammary epithelial cell line for BRCA1 mimicking well the biological defects of known BRCA1 mutant cells, showing a functional link with p53 protein stability, loss of control over regulation of other oncogenes and enhanced tumorigenic potential both in vitro and in vivo. Our in vivo tumor models show that BRCA1 is important in controlling programmed cell death during tumor development, lack of which can lead not only to aggressive growth but also higher levels of VEGF and more vascularization of tumors. This cell line model system may be used to understand the regulation of p53 expression in breast tumorigenesis and to identify the genes promoting breast metastasis. Finally, inhibition of BRCA1 function in this model may also be useful in testing the susceptibility of breast tumors to classical

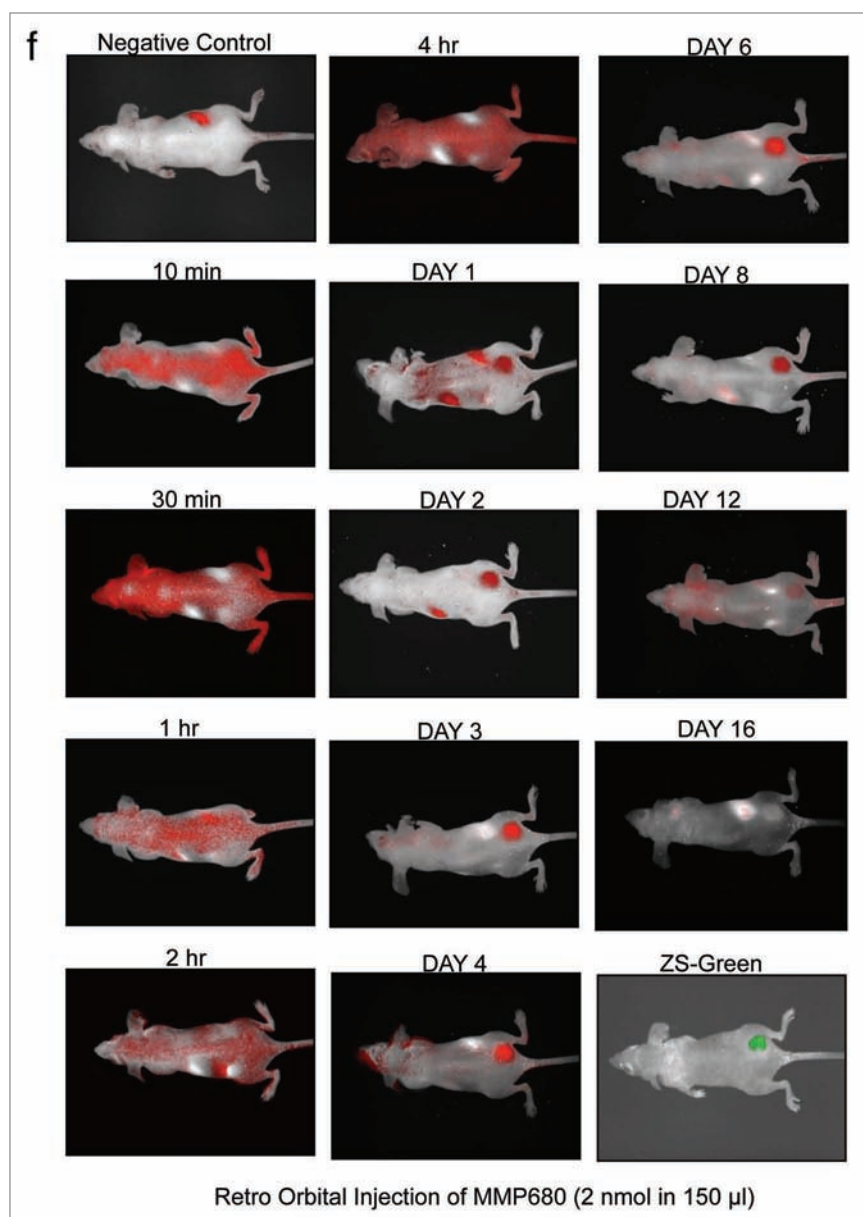


**Figure 4f.** In vivo bio imaging of MMP680 in BRCA1 depleted Ras-transformed MCF10A-Luc tumor xenograft–Maestro. Animals bearing MLBR tumor xenograft was injected retro orbitally with 2 nmol of fluorescent MMP680 probe specific for detecting matrix metallo proteases and imaged regularly using CRi Maestro imaging system. Spectral unmixing was done to separate the signal specific for MMP680 probe in tumor tissues from background auto fluorescence.

chemotherapeutic treatment, anti-angiogenic drug treatment, as well as combinations with DNA repair targeted therapies.

#### Acknowledgements

This work was presented in part at the 97th annual AACR meeting in Washington, D.C. in April, 2006, the 98th annual

AACR meeting in Los Angeles, CA in April, 2007, and at the 99th annual AACR meeting in San Diego, CA in April, 2008. This work was supported in part by NIH grants CA94975, CA105008, and CA123258 to W.S.E-D. This work also received pilot funding in 2006 from the Abramson Cancer Center. W.S.E-D. is an American Cancer Society Research Professor.

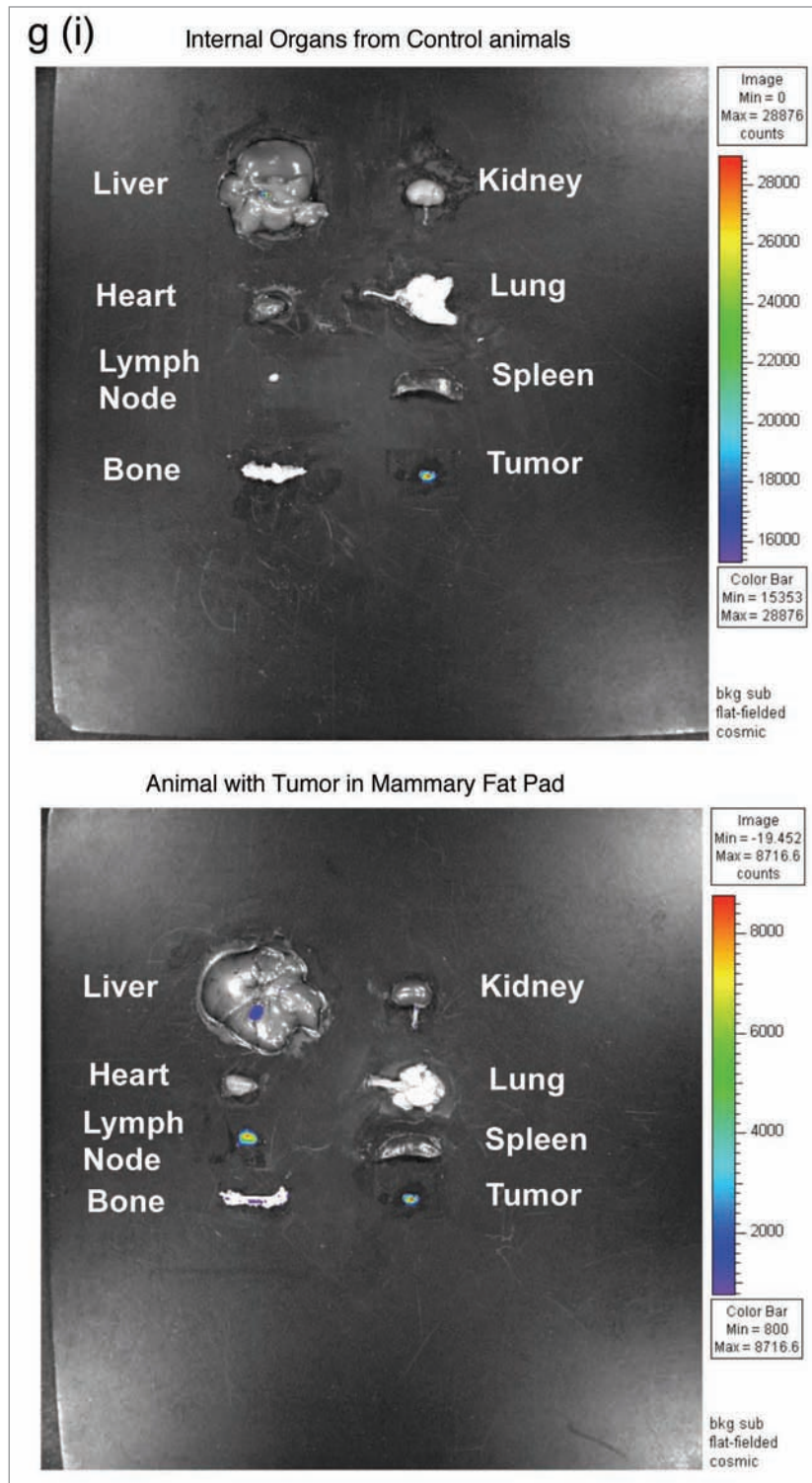


**Figure 4g(i).** Imaging of mouse internal organs for metastasis. Different internal organs were harvested from animals bearing MLBR tumors, nearly after 75 days of tumor cell implantation in mammary fat pads, and imaged for zs-green expression with proper filters either using Xenogen IVIS imaging system (**Fig 4gi**) or CRi Maestro imaging system (**Fig 4gii**). Zs-green detection revealed metastasis of MLBR tumor cells from mammary fat pads to lymph nodes and liver.

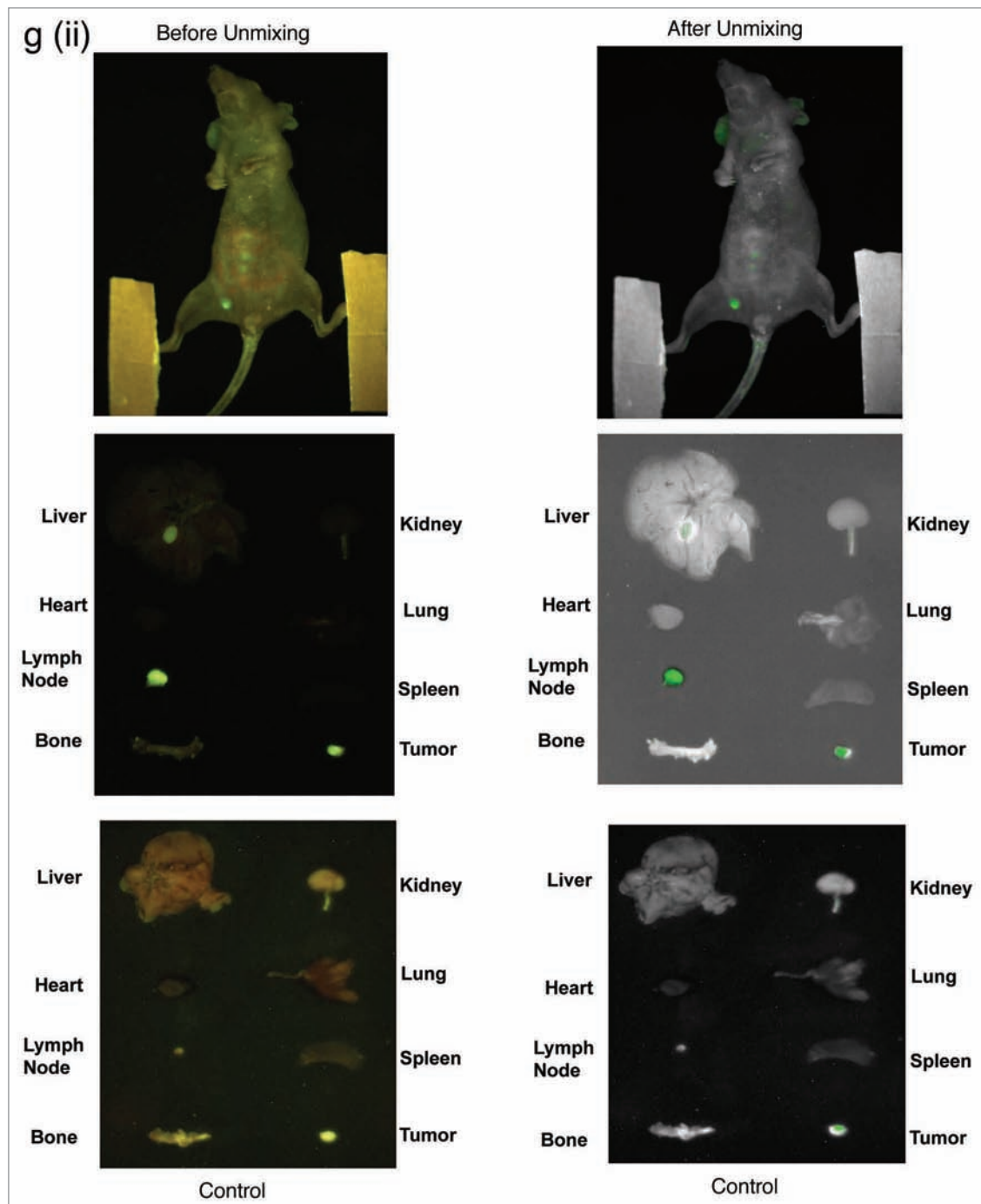


**Figure 4g(ii).** Imaging of mouse internal organs for metastasis. Different internal organs were harvested from animals bearing MLBR tumors, nearly after 75 days of tumor cell implantation in mammary fat pads, and imaged for zs-green expression with proper filters either using Xenogen IVIS imaging system (**Fig 4gi**) or CRi Maestro imaging system (**Fig 4gii**). Zs-green detection revealed metastasis of MLBR tumor cells from mammary fat pads to lymph nodes and liver.

### References

1. Ratsch SB, Gao Q, Srinivasan S, Wazer DE, Band V. Multiple genetic changes are required for efficient immortalization of different subtypes of normal human mammary epithelial cells. *Radiat Res* 2001; 155:143-50.
2. Yaswen P, Stampfer MR. Molecular changes accompanying senescence and immortalization of cultured human mammary epithelial cells. *Int J Biochem Cell Biol* 2002; 34:1382-94.
3. Wazer DE, Liu XL, Chu Q, Gao Q, Band V. Immortalization of distinct human mammary epithelial cell types by human papilloma virus 16 E6 or E7. *Proc Natl Acad Sci U S A* 1995; 92:3687-91.
4. Paulovich AG, Toezyski DP, Hartwell LH. When checkpoints fail. *Cell* 1997; 88:315-21.
5. Sherr CJ. Cancer cell cycles. *Science* 1996; 274:1672-7.
6. Hanahan D, Weinberg RA. The hallmarks of cancer. *Cell* 2000; 100:57-70.
7. Elenbaas B, Spirio L, Koerner F, et al. Human breast cancer cells generated by oncogenic transformation of primary mammary epithelial cells. *Genes Dev* 2001; 15:50-65.
8. Hall JM, Lee MK, Newman B, et al. Linkage of early-onset familial breast cancer to chromosome 17q21. *Science* 1990; 250:1684-9.
9. Miki Y, Swensen J, Shattuck-Eidens D, et al. A strong candidate for the breast and ovarian cancer susceptibility gene BRCA1. *Science* 1994; 266:66-71.

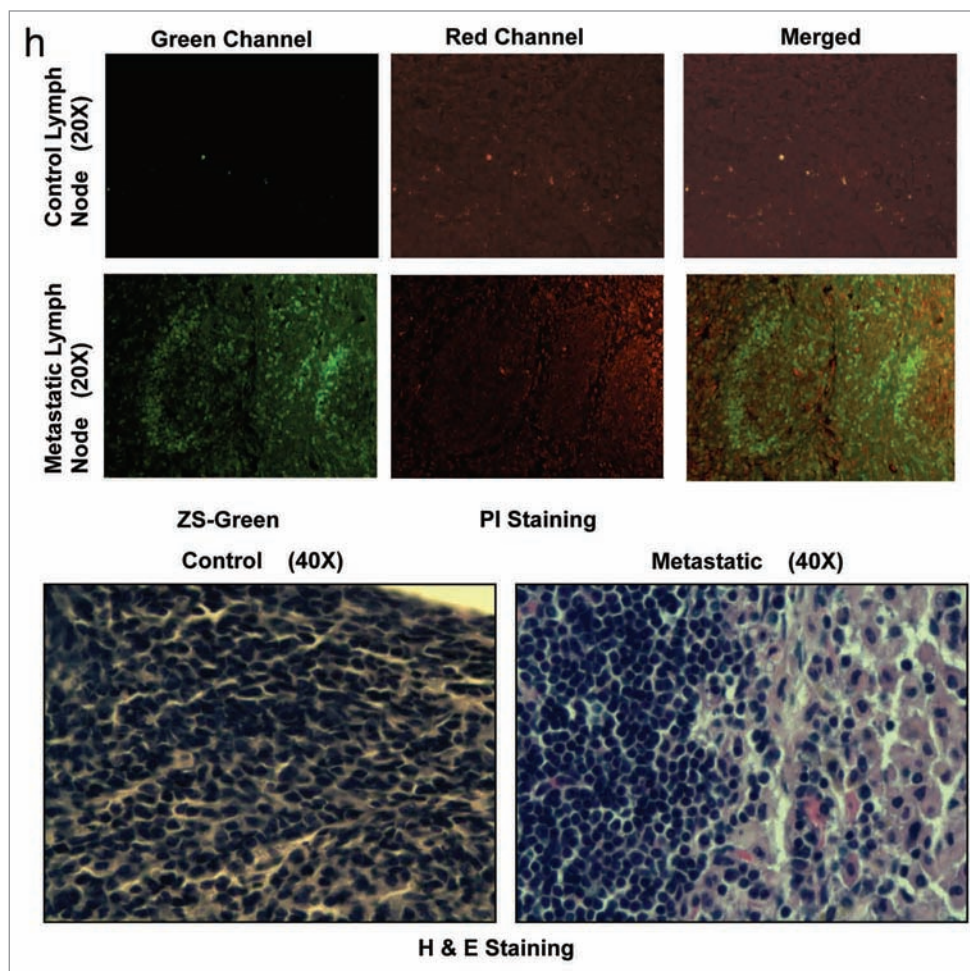


**Figure 4h.** Histological analysis of lymph nodes for metastasis. Paraffin embedded tissue sections of lymph nodes made from animals bearing MLBR tumors in mammary fat pads, were dewaxed before staining with propidium iodide. Fluorescent microscopy scanning of those sections for zs-green confirmed the lymph node metastasis of MLBR tumor cells from its primary site, mammary fat pads. H&E staining revealed the presence of larger sized cells with huge cytoplasm in lymph node, indicative of metastatic MLBR cells.

10. Zheng L, Li S, Boyer TG, Lee WH. Lessons learned from BRCA1 and BRCA2. *Oncogene* 2000; 19:6159-75.
11. Deng CX, Wang RH. Roles of BRCA1 in DNA damage repair: a link between development and cancer. *Hum Mol Genet* 2003; 12 Spec No 1:R113-23.
12. Shen SX, Weaver Z, Xu X, et al. A targeted disruption of the murine Brca1 gene causes gamma-irradiation hypersensitivity and genetic instability. *Oncogene* 1998; 17:3115-24.
13. Ganesan S, Silver DP, Greenberg RA, et al. BRCA1 supports XIST RNA concentration on the inactive X chromosome. *Cell* 2002; 111:393-405.
14. Starita LM, Machida Y, Sankaran S, et al. BRCA1-dependent ubiquitination of gamma-tubulin regulates centrosome number. *Mol Cell Biol* 2004; 24:8457-66.
15. MacLachlan TK, Takimoto R, El-Deiry WS. BRCA1 directs a selective p53-dependent transcriptional response towards growth arrest and DNA repair targets. *Mol Cell Biol* 2002; 22:4280-92.
16. Tomlinson GE, Chen TT, Stastny VA, et al. Characterization of a breast cancer cell line derived from a germ-line BRCA1 mutation carrier. *Cancer Res* 1998; 58:3237-42.
17. Brodie SG, Xu X, Qiao W, Li WM, Cao L, Deng CX. Multiple genetic changes are associated with mammary tumorigenesis in Brca1 conditional knockout mice. *Oncogene* 2001; 20:7514-23.
18. Soule HD, Maloney TM, Wolman SR, et al. Isolation and characterization of a spontaneously immortalized human breast epithelial cell line, MCF-10. *Cancer Res* 1990; 50:6075-86.
19. Furuta S, Jiang X, Gu B, Cheng E, Chen PL, Lee WH. Depletion of BRCA1 impairs differentiation but enhances proliferation of mammary epithelial cells. *Proc Natl Acad Sci U S A* 2005; 102:9176-81.
20. Kim SH, Nakagawa H, Navaraj A, et al. Tumorigenic conversion of primary human esophageal epithelial cells using oncogene combinations in the absence of exogenous Ras. *Cancer Res* 2006; 66:10415-24.
21. Bahnon AB, Dunigan JT, Baysal BE, et al. Centrifugal enhancement of retroviral mediated gene transfer. *J Virol Methods* 1995; 54:131-43.
22. Movassagh M, Boyer O, Burland MC, Leclercq V, Klatzmann D, Lemoine FM. Retrovirus-mediated gene transfer into T cells: 95% transduction efficiency without further in vitro selection. *Hum Gene Ther* 2000; 11:1189-200.
23. Clark EA, Golub TR, Lander ES, Hynes RO. Genomic analysis of metastasis reveals an essential role for RhoC. *Nature* 2000; 406:532-5.
24. Lou Z, Minter-Dykhouse K, Chen J. BRCA1 participates in DNA decatenation. *Nat Struct Mol Biol* 2005; 12:589-93.
25. Hahn WC, Counter CM, Lundberg AS, Beijersbergen RL, Brooks MW, Weinberg RA. Creation of human tumour cells with defined genetic elements. *Nature* 1999; 400:464-8.
26. Weaver VM, Bissell MJ. Functional culture models to study mechanisms governing apoptosis in normal and malignant mammary epithelial cells. *J Mammary Gland Biol Neoplasia* 1999; 4:193-201.
27. Debnath J, Muthuswamy SK, Brugge JS. Morphogenesis and oncogenesis of MCF-10A mammary epithelial acini grown in three-dimensional basement membrane cultures. *Methods* 2003; 30:256-68.
28. Crook T, Crossland S, Crompton MR, Osin P, Gusterson BA. p53 mutations in BRCA1-associated familial breast cancer. *Lancet* 1997; 350:638-9.
29. Berse B, Brown LF, Van de Water L, Dvorak HF, Senger DR. Vascular permeability factor (vascular endothelial growth factor) gene is expressed differentially in normal tissues, macrophages, and tumors. *Mol Biol Cell* 1992; 3:211-20.
30. Leung DW, Cachianes G, Kuang WJ, Goeddel DV, Ferrara N. Vascular endothelial growth factor is a secreted angiogenic mitogen. *Science* 1989; 246:1306-9.
31. Good DJ, Polverini PJ, Rastinejad F, et al. A tumor suppressor-dependent inhibitor of angiogenesis is immunologically and functionally indistinguishable from a fragment of thrombospondin. *Proc Natl Acad Sci U S A* 1990; 87:6624-8.

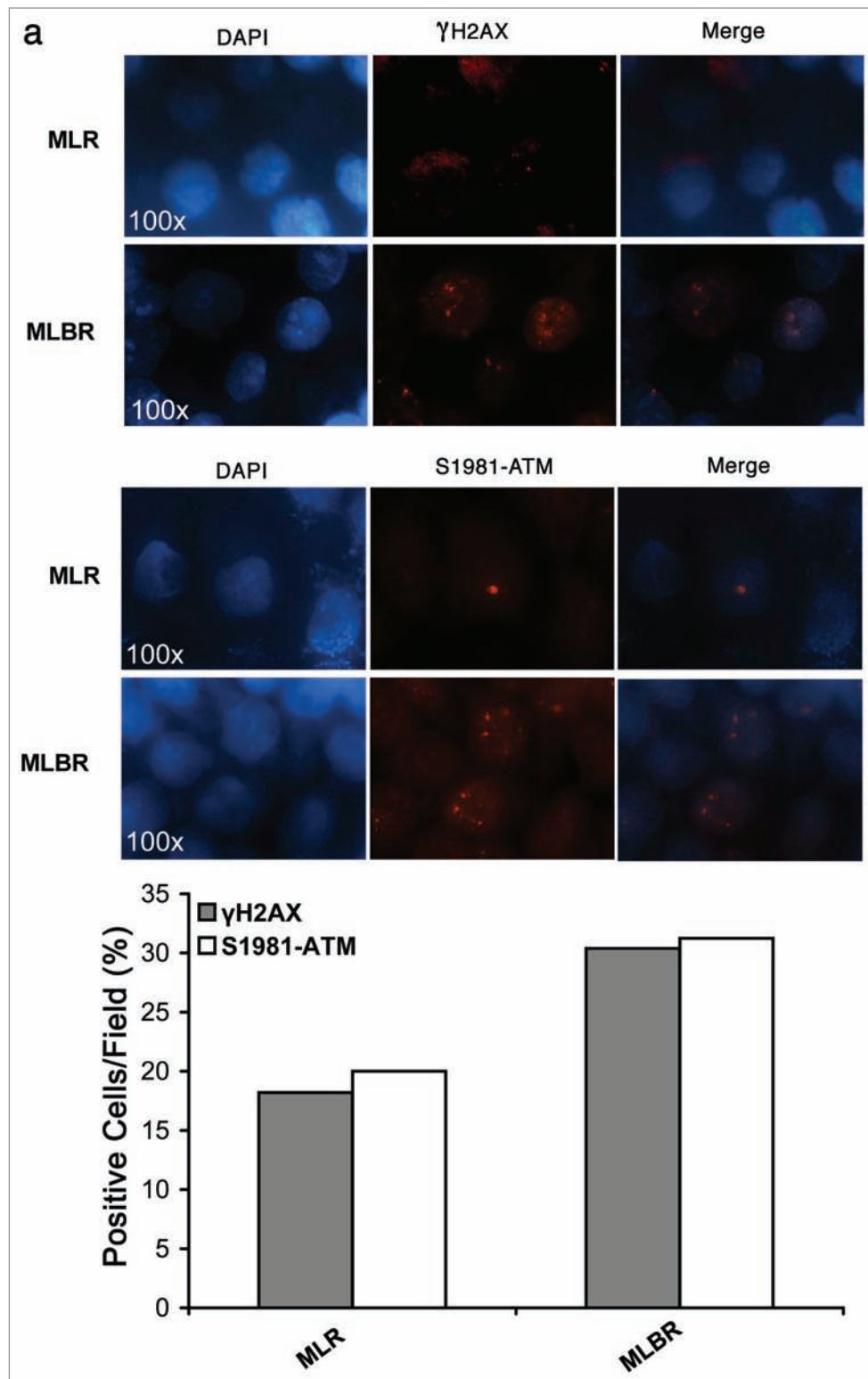


**Figure 5a.** Activation of DNA damage signaling and sensitivity to DNA damaging agents of BRCA1-deficient Ras-transformed human mammary epithelial cells. (5a) Activation of DNA damage signaling in BRCA1-depleted, Ras-transformed MCF10A-Luc cells. Immunocytochemical staining of MLR and MLBR cells with phospho ATM and  $\gamma$ H2AX revealed the presence of double strand breaks and the persistent activation of DNA damage signaling pathways even without any DNA damaging agent treatment.

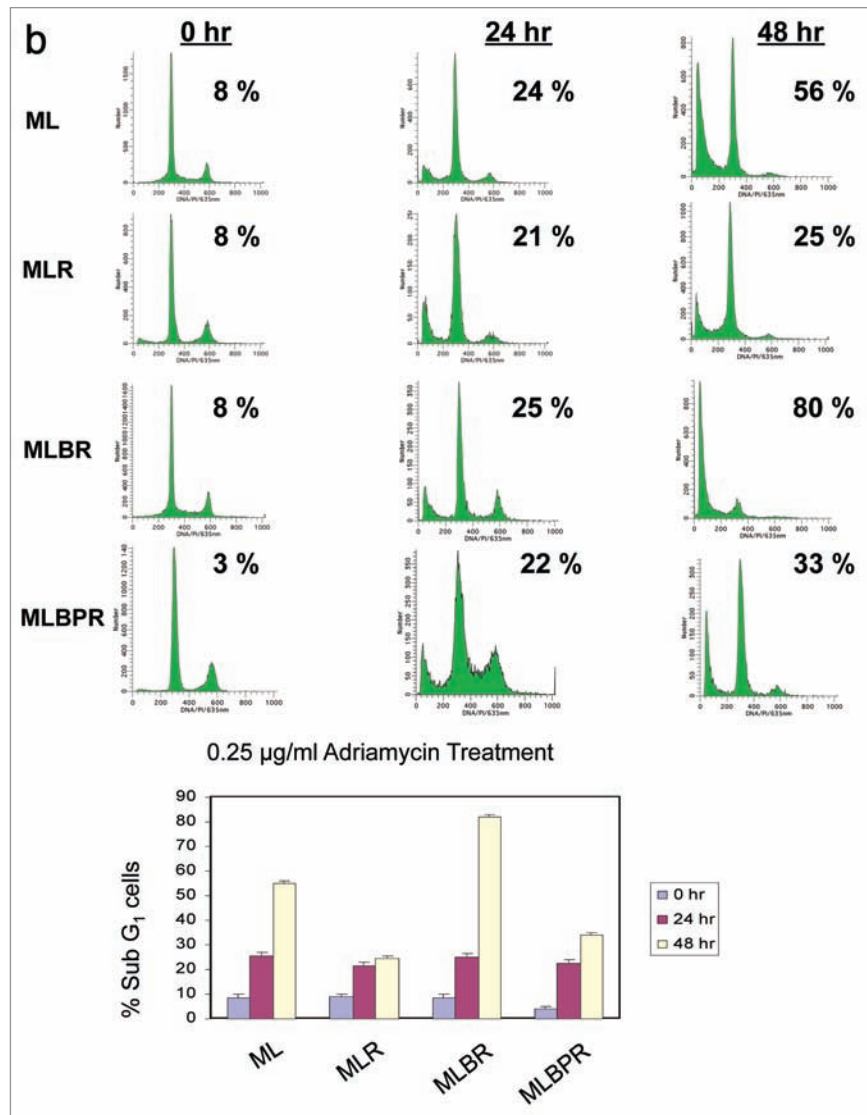


**Figure 5b.** Enhanced sensitivity towards adriamycin in BRCA1-depleted, H-Ras over-expressing MCF10A-Luc cells. Either H-Ras over-expression or p53 depletion provided resistance to transformed MCF10A cells against adriamycin whereas BRCA1 depletion overcame Ras-mediated resistance and sensitized the cells with higher percentage of apoptosis. Average values of three independent experiments were plotted showing an increase in sensitization with BRCA1 depletion.

32. Rak J, Mitsuhashi Y, Bayko L, et al. Mutant ras oncogenes upregulate VEGF/VPF expression: implications for induction and inhibition of tumor angiogenesis. *Cancer Res* 1995; 55:4575-80.
33. Rak J, Mitsuhashi Y, Sheehan C, et al. Oncogenes and tumor angiogenesis: differential modes of vascular endothelial growth factor up-regulation in ras-transformed epithelial cells and fibroblasts. *Cancer Res* 2000; 60:490-8.
34. DeLisser HM, Newman PJ, Albelda SM. Molecular and functional aspects of PECAM-1/CD31. *Immunol Today* 1994; 15:490-5.
35. DeLisser HM, Christofidou-Solomidou M, Strieter RM, et al. Involvement of endothelial PECAM-1/CD31 in angiogenesis. *Am J Pathol* 1997; 151:671-7.
36. Garlanda C, Berthier R, Garin J, et al. Characterization of MEC 14.7, a new monoclonal antibody recognizing mouse CD34: a useful reagent for identifying and characterizing blood vessels and hematopoietic precursors. *Eur J Cell Biol* 1997; 73:368-77.
37. Savagner P, Boyer B, Valles AM, Jouanneau J, Thiery JP. Modulations of the epithelial phenotype during embryogenesis and cancer progression. *Cancer Treat Res* 1994; 71:229-49.
38. Hay ED. An overview of epithelio-mesenchymal transformation. *Acta Anat (Basel)* 1995; 154:8-20.
39. Thiery JP, Chopin D. Epithelial cell plasticity in development and tumor progression. *Cancer Metastasis Rev* 1999; 18:31-42.
40. Thiery JP. Epithelial-mesenchymal transitions in tumour progression. *Nat Rev Cancer* 2002; 2:442-54.
41. Moynahan ME, Chiu JW, Koller BH, Jasin M. Brca1 controls homology-directed DNA repair. *Mol Cell* 1999; 4:511-8.
42. Scully R, Chen J, Ochs RL, et al. Dynamic changes of BRCA1 subnuclear location and phosphorylation state are initiated by DNA damage. *Cell* 1997; 90:425-35.
43. Burma S, Chen BP, Murphy M, Kurimasa A, Chen DJ. ATM phosphorylates histone H2AX in response to DNA double-strand breaks. *J Biol Chem* 2001; 276:42462-7.
44. Moynahan ME, Cui TY, Jasin M. Homology-directed dna repair, mitomycin-c resistance, and chromosome stability is restored with correction of a Brca1 mutation. *Cancer Res* 2001; 61:4842-50.
45. Fan S, Wang J, Yuan R, et al. BRCA1 inhibition of estrogen receptor signaling in transfected cells. *Science* 1999; 284:1354-6.
46. Fan S, Ma YX, Wang C, et al. Role of direct interaction in BRCA1 inhibition of estrogen receptor activity. *Oncogene* 2001; 20:77-87.
47. Yang J, Mani SA, Donaher JL, et al. Twist, a master regulator of morphogenesis, plays an essential role in tumor metastasis. *Cell* 2004; 117:927-39.
48. Hartwell KA, Muir B, Reinhardt F, Carpenter AE, Sgroi DC, Weinberg RA. The Spemann organizer gene, Gooseoid, promotes tumor metastasis. *Proc Natl Acad Sci USA* 2006; 103:18969-74.
49. Batlle E, Sancho E, Franci C, et al. The transcription factor snail is a repressor of E-cadherin gene expression in epithelial tumour cells. *Nat Cell Biol* 2000; 2:84-9.

50. Cano A, Perez-Moreno MA, Rodrigo I, et al. The transcription factor snail controls epithelial-mesenchymal transitions by repressing E-cadherin expression. *Nat Cell Biol* 2000; 2:76-83.
51. Carver EA, Jiang R, Lan Y, Oram KF, Gridley T. The mouse snail gene encodes a key regulator of the epithelial-mesenchymal transition. *Mol Cell Biol* 2001; 21:8184-8.
52. Nieto MA, Sargent MG, Wilkinson DG, Cooke J. Control of cell behavior during vertebrate development by Slug, a zinc finger gene. *Science* 1994; 264:835-9.
53. Savagner P, Yamada KM, Thiery JP. The zinc-finger protein slug causes desmosome dissociation, an initial and necessary step for growth factor-induced epithelial-mesenchymal transition. *J Cell Biol* 1997; 137:1403-19.
54. Comijn J, Berx G, Vermassen P, et al. The two-handed E box binding zinc finger protein SIP1 downregulates E-cadherin and induces invasion. *Mol Cell* 2001; 7:1267-78.
55. Mani SA, Yang J, Brooks M, et al. Mesenchyme Forkhead 1 (FOXC2) plays a key role in metastasis and is associated with aggressive basal-like breast cancers. *Proc Natl Acad Sci USA* 2007; 104:10069-74.
56. Ma L, Teruya-Feldstein J, Weinberg RA. Tumour invasion and metastasis initiated by microRNA-10b in breast cancer. *Nature* 2007; 449:682-8.
57. Huang Q, Gumireddy K, Schrier M, et al. The microRNAs miR-373 and miR-520c promote tumour invasion and metastasis. *Nat Cell Biol* 2008; 10:202-10.
58. Zhong Q, Chen CF, Li S, et al. Association of BRCA1 with the hRad50-hMre11-p95 complex and the DNA damage response. *Science* 1999; 285:747-50.
59. Cortez D, Wang Y, Qin J, Elledge SJ. Requirement of ATM-dependent phosphorylation of brca1 in the DNA damage response to double-strand breaks. *Science* 1999; 286:1162-6.
60. Scully R, Chen J, Plug A, et al. Association of BRCA1 with Rad51 in mitotic and meiotic cells. *Cell* 1997; 88:265-75.